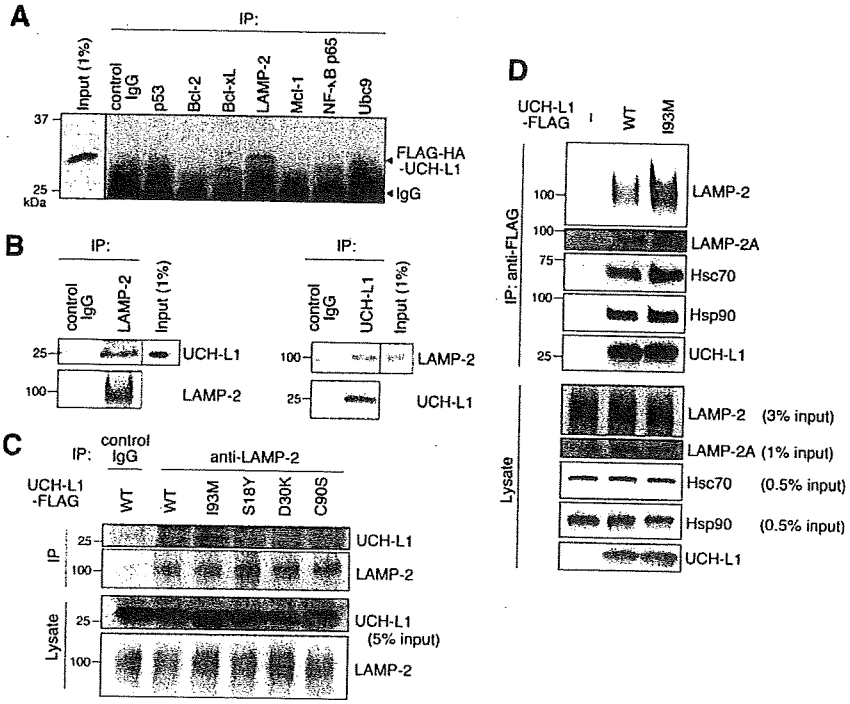

FIGURE 1. **Physical interactions of UCH-L1 with LAMP-2A, Hsc70, and Hsp90.** *A*, lysates of NIH-3T3 cells stably expressing FLAG-hemagglutinin (*HA*)-tagged UCH-L1 were immunoprecipitated (*IP*) with antibodies against cell death- or protein degradation-related proteins and analyzed by immunoblotting using anti-UCH-L1 antibody. A representative blot including immunoprecipitant with anti-LAMP-2 antibody is shown. *B*, mouse (C57BL/6J) whole brain lysates were immunoprecipitated with control IgG, anti-LAMP-2, or anti-UCH-L1 antibody and immunoblotted with anti-UCH-L1 and LAMP-2 antibodies. *C*, lysates of COS-7 cells transfected with the indicated constructs were immunoprecipitated with 5 μg/ml control IgG or anti-LAMP-2 antibody and analyzed by immunoblotting using anti-UCH-L1 antibody. *D*, lysates of COS-7 cells transfected with the indicated constructs (−, empty vector) were immunoprecipitated with anti-FLAG beads and immunoblotted using anti-LAMP2, LAMP-2A, Hsc70, Hsp90, and UCH-L1 antibodies.

points after the suppression of the gene and analyzed by immunoblotting. Pulse-chase analyses were performed as described previously (21) with some modifications. COS-7 cells transfected with pCI-neo-hUCH-L1-FLAG were washed and incubated with methionine-, cysteine-, and cystine-free medium for 1 h. The cells were pulsed with 0.1 mCi/ml [^{35}S]Met and [^{35}S]Cys (Expre^{35}S^{35}S protein labeling mixture, PerkinElmer Life Sciences) for 1 h and then washed and chased with 3 mM methionine and cysteine for 48 h. At the 0-, 24-, and 48-h time points, the cells were harvested for immunoprecipitation with anti-FLAG M2 affinity gel. Following SDS-PAGE on a 15% gel, radioactive bands were detected and analyzed by using a BAS-5000 imaging analyzer (Fujifilm, Tokyo, Japan).

Statistical Analysis—For comparison of two groups, the statistical significance of differences was determined by the Student's *t* test.

RESULTS

UCH-L1 Interacts with LAMP-2A, Hsc70, and Hsp90—We have previously shown that soluble UCH-L1 interacts with multiple proteins in mammalian cells and that one of the UCH-L1-interacting proteins is α/β-tubulin (13). In this study, we further screened for UCH-L1-interacting proteins using a coimmunoprecipitation assay (Fig. 1*A*). We identified LAMP-2 as a novel UCH-L1-interacting protein (Fig. 1*A*). To confirm this interaction *in vivo*, a coimmunoprecipitation assay was performed using mouse whole brain lysate. Interaction between endogenous UCH-L1 and endogenous LAMP-2 was observed (Fig. 1*B*). LAMP-2 exists in three different isoforms, LAMP-2A, LAMP-2B, and LAMP-2C, which are produced by the alternative splicing of the LAMP-2 pre-mRNA (31). LAMP-2A forms a complex with chaperones such as Hsc70 and Hsp90 and functions as a receptor for CMA at the lysosomal membrane (26). Because α-synuclein has been reported to interact with LAMP-2A (24), we tested for interactions between UCH-L1 and LAMP-2A, Hsc70, and Hsp90. The UCH-L1 immunoprecipitant included LAMP-2A as well as Hsc70 and Hsp90 (Fig. 1*D*). These results indicate that UCH-L1 interacts with LAMP-2A, Hsc70, and Hsp90 in mammalian cells.

UCH-L1 Can Be Degraded by Macroautophagy—Although UCH-L1 physically interacts with LAMP-2A, UCH-L1 is not a presumable substrate for CMA because UCH-L1 does not contain a KFERQ-like motif, which is required for substrate proteins to be degraded by CMA (32). Therefore, we speculated that UCH-L1 is degraded by other degradation pathways in mammalian cells. We used a regulatory protein expression system to switch off the expression of UCH-L1 by adding doxycycline, to follow UCH-L1 degradation. Degradation of UCH-L1 was observed 24 or 48 h after expression was switched off, compared with the time point at which expression was switched off (Fig. 2*A*). The half-life of UCH-L1 was >48 h (Fig. 2*A*). Long-lived proteins are known to be mainly degraded by macroautophagy (33). We therefore investigated whether UCH-L1 was degraded by macroautophagy using 3-MA, an inhibitor of macroautophagy (24, 28, 34). The 3-MA treatment significantly inhibited the degradation of UCH-L1 (Fig. 2*A*). Similar results were obtained when we used UCH-L1^{I93M} (Fig. 2*B*). Pulse-chase experiments also showed that the degradations of UCH-L1^{WT} and UCH-L1^{I93M} were significantly inhibited by 3-MA treatment (Fig. 2, *C* and *D*). These results suggest that macroautophagy is one of the major pathways that degrade UCH-L1 in our cell model.

The Interactions of UCH-L1 with LAMP-2A, Hsc70, and Hsp90 Are Enhanced by the I93M Mutation in UCH-L1 and Are Independent of the Interaction between Monoubiquitin and

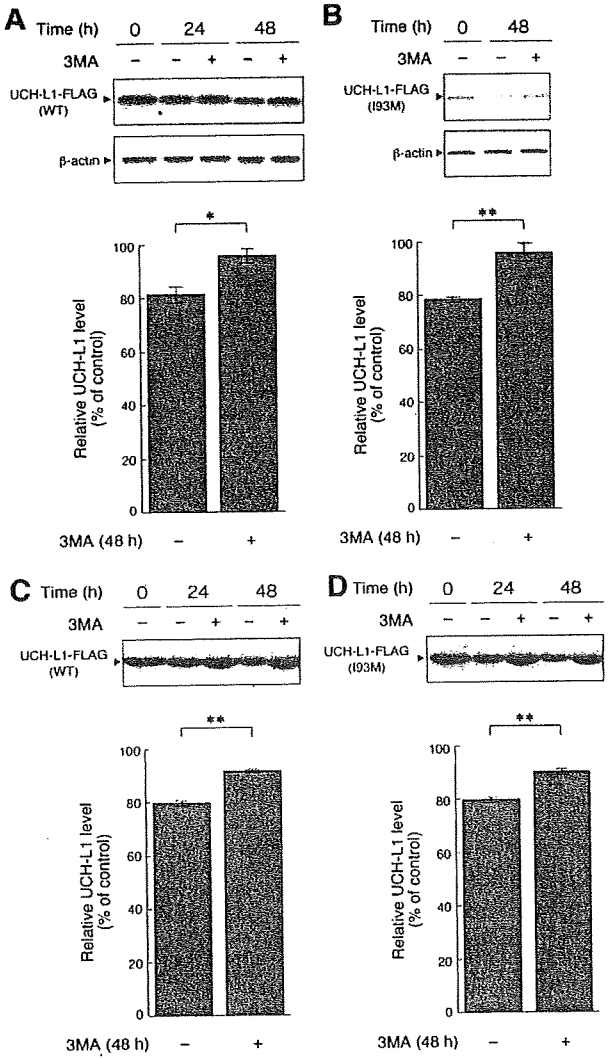

FIGURE 2. **Degradation of UCH-L1 by macroautophagy.** *A* and *B*, COS-7 cells were transfected with pTet-Off and pTRE-Tight-hUCH-L1^{WT} (*A*) or pTRE-Tight-hUCH-L1^{I93M} (*B*). Twenty-four h after transfection, transcription of UCH-L1-FLAG gene was suppressed by adding 100 ng/ml doxycycline and incubating for 4 h. Then, 3-MA (+) or vehicle (−) was added, and cells were harvested at the indicated times after the suppression of the gene and analyzed by immunoblotting (*upper panels*). The relative levels of UCH-L1-FLAG at 48 h after the suppression (% of 0-h control) were quantified by densitometry. Mean values are shown with S.E. (*A*, $n = 4$; *B*, $n = 3$). *, $p < 0.05$; **, $p < 0.01$. *C* and *D*, COS-7 cells were transfected with pCI-neo-hUCH-L1^{WT}-FLAG (*C*) or pCI-neo-hUCH-L1^{I93M}-FLAG (*D*). Twenty-four h after transfection, cells were labeled with [^{35}S]Met and [^{35}S]Cys. Autoradiograms of anti-FLAG immunoprecipitates pulse-chased at the indicated times in the absence or presence of 3-MA are shown (*upper panels*). Relative band intensities at 48 h (% of 0-h control) are quantified. Mean values are shown with S.E. ($n = 3$). **, $p < 0.01$.

UCH-L1—We have previously shown that the amount of each protein interacting with UCH-L1^{I93M} is mostly higher than the amount interacting with UCH-L1^{WT} (13). Consistent with this observation, we found that the amount of LAMP-2A, Hsc70, and Hsp90 interacting with UCH-L1^{I93M} is higher than the amount interacting with UCH-L1^{WT} (~1.8-, 1.3-, and 1.3-fold increases, respectively) (Fig. 1, *C* and *D*, and supplemental Fig. S2*A*). The interactions of LAMP-2, Hsc70, or Hsp90 with UCH-L1^{S18Y}, UCH-L1^{D30K}, which lacks hydrolase activity and binding affinity for ubiquitin (21), and UCH-L1^{C90S}, which lacks hydrolase activity but maintains binding affinity for ubiquitin (21), were not notably changed compared with those of UCH-L1^{WT} (Fig. 1*C*, supplemental Fig. S2*A*, and data not shown). These results suggest that the interaction between UCH-L1 and CMA machinery is independent of both UCH-L1-binding affinity for ubiquitin and the hydrolase activity of UCH-L1. To further show that these interactions are independent of monoubiquitin binding to UCH-L1, and to elucidate the amino acid residues of UCH-L1 involved in the interaction with LAMP-2A, Hsc70, and Hsp90, we performed coimmunoprecipitation assays using a series of alanine substitutions (13) of basic and acidic residues located on the surface of UCH-L1 (Fig. 3*A*). The R63A mutant displayed increased levels of interactions with LAMP-2, Hsc70, and Hsp90, whereas other mutations had no notable effect on the interactions (Fig. 3*A*). We further performed alanine-scanning mutagenesis experiments and found that E174A, D176A, and H185A mutants also displayed increased levels of interactions with LAMP-2, Hsc70, and Hsp90 (Fig. 3*B* and data not shown). Glu^{174}, Asp^{176}, and His^{185} are located near Arg^{63} (Fig. 3*C*). The surface region containing Arg^{63} and His^{185} possesses features that are characteristic of a protein-protein interacting site (35). These observations suggest that this surface region, which is distinct from the ubiquitin-binding region (13, 35), is involved in the interactions with LAMP-2, Hsc70, and Hsp90. The R63A, E174A, D176A, or H185A mutation possibly causes partial misfolding, resulting in increased interactions.

UCH-L1 Directly Interacts with the Cytoplasmic Region of LAMP-2A—LAMP-2 is a type 1 membrane protein, consisting of a short cytoplasmic tail (12 amino acids), one transmembrane domain, and a glycosylated luminal domain (31). To test whether UCH-L1 directly interacts with the cytosolic region of LAMP-2A, we prepared purified recombinant wild-type and I93M UCH-L1 proteins, a peptide containing an amino acid sequence corresponding to the C-terminal cytoplasmic tail of LAMP-2A, and a control peptide (Fig. 4*A*). Purified UCH-L1 proteins and the peptides were mixed, and pulldown assays were performed. A direct interaction between wild-type UCH-L1 and the cytosolic region of LAMP-2A was observed (Fig. 4, *B* and *C*). Consistent with the results of the coimmunoprecipitation assay, UCH-L1^{I93M} exhibited an abnormally increased level of interaction with the cytosolic region of LAMP-2A compared with wild-type UCH-L1 (Fig. 4*D*). Because chaperones, including Hsc70, are considered to be required for the interaction of the CMA substrates with LAMP-2A (36), our results may indicate that UCH-L1 interacts with LAMP-2A in a manner different from the interaction between CMA substrates and LAMP-2A.

UCH-L1^{I93M} Causes Accumulation of α-Synuclein—It has been reported that α-synuclein^{WT} is a CMA substrate, but pathogenic mutants A30P and A53T α-synuclein inhibit CMA by tight binding to LAMP-2A (24). Thus, UCH-L1^{I93M}, which exhibits elevated interactions with LAMP-2A, Hsc70, and Hsp90, may also inhibit CMA. To examine this possibility in mammalian cells, we assessed the effects of UCH-L1^{I93M} on the

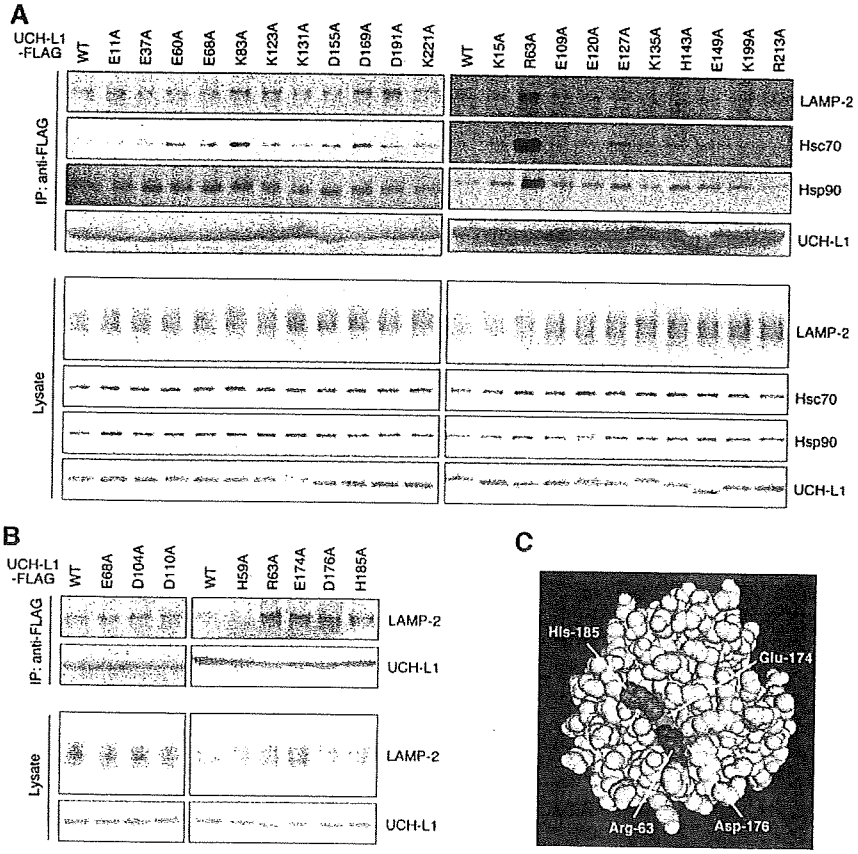

FIGURE 3. **Alanine-scanning mutagenesis of UCH-L1.** *A* and *B*, lysates of COS-7 cells transfected with the indicated constructs were immunoprecipitated (*IP*) with anti-FLAG antibody and analyzed by immunoblotting. *C*, a structural model for human UCH-L1 is shown. Arg^{63}, Glu^{174}, Asp^{176}, and His^{185} are shown in *blue*, *green*, *magenta*, and *red*, respectively, using Cn3D software (version 4.1) and NCBI structural model mmdbId:38174 (35).

protein level of GAPDH, an established substrate of CMA (24), in the lysosomal fraction and whole-cell lysate. The GAPDH level in whole-cell lysate was increased in cells expressing UCH-$L1^{I93M}$ compared with that in cells expressing UCH-$L1^{WT}$ (an ~1.5-fold increase) (Fig. 5*A*), whereas the GAPDH level in the lysosomal fraction was decreased in cells expressing UCH-$L1^{I93M}$ (an ~2.1-fold decrease) (Fig. 5*B*), supporting the idea that the aberrant interaction of UCH-$L1^{I93M}$ with CMA machinery inhibits CMA. The inhibition of CMA also results in the accumulation of other CMA substrates, including α-synuclein (24). We found that the amount of α-$synuclein^{WT}$ was increased in cells expressing UCH-$L1^{I93M}$ compared with cells expressing UCH-$L1^{WT}$ (~1.7 and 1.4-fold increases, respectively) (Fig. 5, *C* and *D*) or control mock cells (data not shown). The physical interaction between UCH-L1 and α-synuclein was not detected under these experimental conditions (data not shown). These results suggest that the accumulation of α-synuclein in cells expressing UCH-$L1^{I93M}$ is due to the inhibition of CMA-dependent degradation of α-synuclein. α-Synuclein contains a CMA recognition motif, ^{95}VKKDQ^{99}, and mutant α-$synuclein^{\Delta DQ}$, in which ^{98}DQ^{99} is replaced by Ala-Ala, is not degraded by CMA (24). To confirm that the accumulation of α-synuclein in cells expressing UCH-$L1^{I93M}$ is associated with CMA-dependent degradation of α-synuclein, we used mutant α-$synuclein^{\Delta DQ}$ and found that the I93M mutation does not affect the α-$synuclein^{\Delta DQ}$ level (~1.0 and 1.0-fold increases, respectively) (Fig. 5, *E* and *F*).

G93A Cu,Zn-superoxide dismutase 1 and WT Cu,Zn-superoxide dismutase 1 are not presumable substrates for CMA because Cu,Zn-superoxide dismutase 1 does not contain a KFERQ-like motif, but they can be degraded by the proteasome and macroautophagy (28). Protein levels of G93A Cu,Zn-superoxide dismutase 1 and WT Cu,Zn-superoxide dismutase 1 in cells transfected with UCH-$L1^{I93M}$ were not increased compared with those in cells expressing UCH-$L1^{WT}$ (an ~1.0-fold increase) (Fig. 5*G* and data not shown), suggesting that the I93M mutation does not considerably affect the degradation of proteins by macroautophagy and the proteasome under these experimental conditions.

Contrary to UCH-$L1^{I93M}$, UCH-$L1^{D30K}$ and UCH-$L1^{C90S}$ did not increase the amount of α-synuclein in cells (supplemental Fig. S2*B*), indicating that the accumulation of α-synuclein in cells expressing UCH-$L1^{I93M}$ is independent of the hydrolase activity of UCH-L1 and the interaction between monoubiquitin and UCH-L1. These observations are consistent with the results showing that the interaction between UCH-L1 and LAMP-2A, Hsc70, or Hsp90 is independent of the enzymatic activity of UCH-L1 and the interaction between monoubiquitin and UCH-L1 (Figs. 1*C* and 3) and also with the idea that the main cause of UCH-$L1^{I93M}$-associated PD is not a loss of UCH-L1 function but an acquired toxicity of UCH-$L1^{I93M}$.

DISCUSSION

An increase in the amount of α-synuclein protein could constitute a pathogenic factor underlying sporadic PD because the heterozygous duplication of the α-synuclein gene causes familial PD (4, 5), and the deposition of α-synuclein protein is associated with sporadic PD (7, 8, 37). α-$Synuclein^{WT}$ is a CMA substrate, but mutant A30P and A53T α-synuclein inhibit CMA by aberrant tight binding to LAMP-2A (24). Thus, inhibition of CMA by mutant α-synuclein might result in an increase in the amount of α-synuclein protein, leading to the neurodegeneration in familial PD associated with mutant α-synuclein. To date, the relationships between α-synuclein and other familial PD-

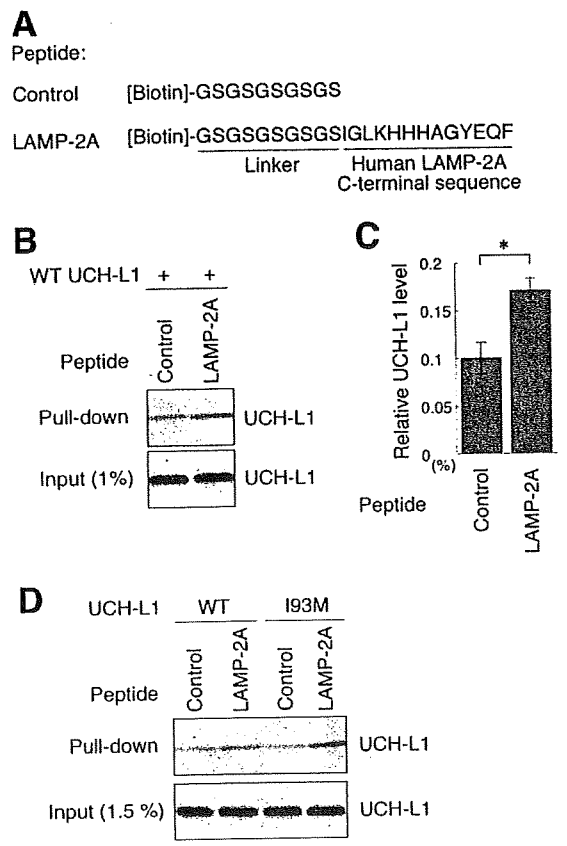

FIGURE 4. **Direct interaction between UCH-L1 and the cytosolic region of LAMP-2A.** *A*, an amino acid sequence of biotin-conjugated peptides is shown. *B* and *C*, 10 μg of recombinant UCH-L1 and 2 nmol of peptides (control or LAMP-2A peptide) were mixed, and a pulldown assay was performed using streptavidin beads. Precipitants were analyzed by immunoblotting (*B*). The levels of UCH-L1 relative to input were quantified by densitometry. Mean values are shown with S.E. ($n = 3$). *, $p < 0.05$. *D*, 10 μg of UCH-L1 (wild-type or I93M) and 2 nmol of peptides (control or LAMP-2A peptide) were mixed, and a pulldown assay was performed.

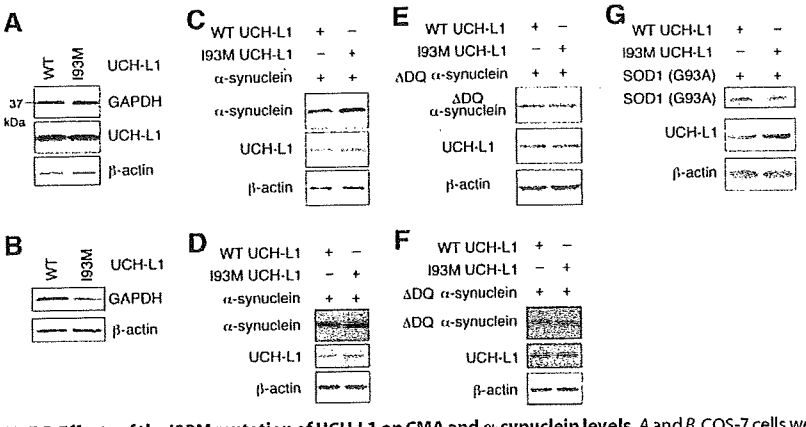

FIGURE 5. **Effects of the I93M mutation of UCH-L1 on CMA and α-synuclein levels.** *A* and *B*, COS-7 cells were transfected with the indicated constructs. Forty-eight h after transfection, whole-cell lysates (*A*) and a lysosomal fraction (*B*) were prepared and analyzed by immunoblotting. *C–G*, COS-7 cells (*C*, *E*, and *G*) or IMR-90 cells (*D* and *F*) were transfected with the indicated constructs. Cell lysates were prepared and analyzed by immunoblotting. Accumulation of α-synuclein^{WT} in cells transfected with UCH-L1^{I93M} was observed in COS-7 (*C*), IMR-90 (*D*), and SH-SY5Y cells (data not shown). The assays were performed at least three times; representative results are shown. *SOD1*, Cu,Zn-superoxide dismutase 1.

associated mutant proteins in the pathogenesis of PD have remained largely unclear. Although it was reported that UCH-L1 polyubiquitinates monoubiquitinated α-synuclein in a cell-free system (20), the relationship between UCH-L1 and non-ubiquitinated α-synuclein in the pathogenesis of PD has also remained unknown.

In the present study, we have shown that familial PD-associated UCH-L1^{I93M} abnormally interacts with LAMP-2A, Hsc70, and Hsp90 and causes an increase in the amounts of α-synuclein and GAPDH, which are CMA substrates, in cultured cells. The increase can be explained by an inhibition of CMA via an aberrant interaction between UCH-L1^{I93M} and CMA machinery because the GAPDH level in the lysosomal fraction was decreased in cells expressing UCH-L1^{I93M} (Fig. 5*B*), and the I93M mutation in UCH-L1 does not affect the levels of α-synuclein$^{\Delta DQ}$, which is not degraded by CMA (Fig. 5, *E* and *F*). These findings suggest that an increase in the amount of α-synuclein protein by inhibition of CMA via the interaction between UCH-L1^{I93M} and CMA machinery underlies one of the causes of familial PD associated with mutant UCH-L1. It is also possible that increases in the amount of other CMA substrates, such as GAPDH, are involved in the pathogenesis of PD. Taken together with a report that pathogenic mutant A30P and A53T α-synuclein exhibit an enhanced interaction with LAMP-2A compared with α-synuclein^{WT} (24), our results indicate that UCH-L1^{I93M} and mutant A30P and A53T α-synuclein share aberrant biochemical properties with respect to their interactions with LAMP-2A. These observations further support the idea that the I93M mutation in UCH-L1 contributes to the pathogenesis of PD.

We revealed that the R63A, E174A, D176A, or H185A substitution in UCH-L1 increases the levels of interactions of UCH-L1 with LAMP-2, Hsc70, and Hsp90 (Fig. 3), suggesting that the surface region containing Arg^{63} and His^{185} in UCH-L1 (35) is involved in its interaction with LAMP-2, Hsc70, and Hsp90. We have previously reported that the R63A or H185A substitution in UCH-L1 enhances the interaction of UCH-L1 with tubulin (13). These results suggest that tubulin, LAMP-2A, Hsc70, and Hsp90 interact with the same region in UCH-L1. Arg^{63} and His^{185} are distinct from Asp^{30}, which is one of the ubiquitin-binding sites (21, 38), and from Cys^{90} (13), which is a catalytic center cysteine residue. We have shown that D30K or C90S mutation in UCH-L1 does not alter its interactions with tubulin (13) and LAMP-2 (Fig. 1*C*). Thus, the interactions of UCH-L1 with tubulin and LAMP-2 are independent of the monoubiquitin-binding and hydrolase activity of UCH-L1.

It is known that the majority of PD cases occur sporadically and that oxidative/carbonyl stresses are

elevated in PD brains (17, 39). In the brains of sporadic PD patients, UCH-L1 is a major target of carbonyl formation (17). We previously reported that carbonyl-modified UCH-L1 and UCH-L1^{I93M} share biochemical properties: both of these UCH-L1 variants display increased insolubility, elevated interactions with multiple proteins including tubulin, and decreased interaction with monoubiquitin compared with UCH-L1^{WT} (13). We have also shown that both carbonyl-modified UCH-L1 and UCH-L1^{I93M} abnormally promote tubulin polymerization (13). Our previous studies using circular dichroism suggest that both of these UCH-L1 variants display decreased α-helix and increased β-sheet content (13, 22, 40). Thus, both carbonyl modification and the I93M mutation in UCH-L1 may alter its conformation, resulting in changes in the biochemical and functional properties of UCH-L1. It is an interesting issue whether carbonyl-modified UCH-L1 can also inhibit CMA. Other than tubulin, LAMP-2A, Hsc70, and Hsp90, UCH-L1 interacts with multiple proteins (13). These other interactors may also be involved in the mechanism of UCH-L1-mediated PD and are currently under investigation. It is also possible that the interaction of Hsc70 or Hsp90 with UCH-L1 plays roles other than in the CMA pathway.

α-Synuclein and UCH-L1 have been reported to be expressed abundantly in dopaminergic neurons in the human brain (41). Thus, UCH-L1^{I93M} is possibly overproduced in dopaminergic neurons in familial PD, leading to an accumulation of α-synuclein and the selective loss of dopaminergic neurons. In conclusion, familial PD-associated mutant UCH-L1^{I93M} physically interacts with LAMP-2A, Hsc70, and Hsp90 and causes an increase in the amount of α-synuclein in cells. We propose that aberrant interaction of mutant UCH-L1 with CMA machinery, at least in part, underlies the pathogenesis of familial PD associated with UCH-L1^{I93M}.

Acknowledgments—We thank Dr. Yasuyuki Suzuki (National Institute of Neuroscience) and Dr. Rieko Setsuie (National Institute of Neuroscience) for scientific comments and Takeshi Mitsui (National Institute of Neuroscience) for technical assistance.

REFERENCES

1. Polymeropoulos, M. H., Lavedan, C., Leroy, E., Ide, S. E., Dehejia, A., Dutra, A., Pike, B., Root, H., Rubenstein, J., Boyer, R., Stenroos, E. S., Chandrasekharappa, S., Athanassiadou, A., Papapetropoulos, T., Johnson, W. G., Lazzarini, A. M., Duvoisin, R. C., Di Iorio, G., Golbe, L. I., and Nussbaum, R. L. (1997) *Science* **276,** 2045–2047
2. Kruger, R., Kuhn, W., Muller, T., Woitalla, D., Graeber, M., Kosel, S., Przuntek, H., Epplen, J. T., Schols, L., and Riess, O. (1998) *Nat. Genet.* **18,** 106–108
3. Zarranz, J. J., Alegre, J., Gomez-Esteban, J. C., Lezcano, E., Ros, R., Ampuero, I., Vidal, L., Hoenicka, J., Rodriguez, O., Atares, B., Llorens, V., Gomez Tortosa, E., del Ser, T., Munoz, D. G., and de Yebenes, J. G. (2004) *Ann. Neurol.* **55,** 164–173
4. Chartier-Harlin, M. C., Kachergus, J., Roumier, C., Mouroux, V., Douay, X., Lincoln, S., Levecque, C., Larvor, L., Andrieux, J., Hulihan, M., Waucquier, N., Defebvre, L., Amouyel, P., Farrer, M., and Destee, A. (2004) *Lancet* **364,** 1167–1169
5. Ibanez, P., Bonnet, A. M., Debarges, B., Lohmann, E., Tison, F., Pollak, P., Agid, Y., Durr, A., and Brice, A. (2004) *Lancet* **364,** 1169–1171
6. Singleton, A. B., Farrer, M., Johnson, J., Singleton, A., Hague, S., Kachergus, J., Hulihan, M., Peuralinna, T., Dutra, A., Nussbaum, R., Lincoln, S., Crawley, A., Hanson, M., Maraganore, D., Adler, C., Cookson, M. R., Muenter, M., Baptista, M., Miller, D., Blancato, J., Hardy, J., and Gwinn-Hardy, K. (2003) *Science* **302,** 841
7. Spillantini, M. G., Schmidt, M. L., Lee, V. M., Trojanowski, J. Q., Jakes, R., and Goedert, M. (1997) *Nature* **388,** 839–840
8. Spillantini, M. G., Crowther, R. A., Jakes, R., Hasegawa, M., and Goedert, M. (1998) *Proc. Natl. Acad. Sci. U. S. A.* **95,** 6469–6473
9. Leroy, E., Boyer, R., Auburger, G., Leube, B., Ulm, G., Mezey, E., Harta, G., Brownstein, M. J., Jonnalagada, S., Chernova, T., Dehejia, A., Lavedan, C., Gasser, T., Steinbach, P. J., Wilkinson, K. D., and Polymeropoulos, M. H. (1998) *Nature* **395,** 451–452
10. Setsuie, R., and Wada, K. (2007) *Neurochem. Int.* **51,** 105–111
11. Healy, D. G., Abou-Sleiman, P. M., and Wood, N. W. (2004) *Cell Tissue Res.* **318,** 189–194
12. Setsuie, R., Wang, Y. L., Mochizuki, H., Osaka, H., Hayakawa, H., Ichihara, N., Li, H., Furuta, A., Sano, Y., Sun, Y. J., Kwon, J., Kabuta, T., Yoshimi, K., Aoki, S., Mizuno, Y., Noda, M., and Wada, K. (2007) *Neurochem. Int.* **50,** 119–129
13. Kabuta, T., Setsuie, R., Mitsui, T., Kinugawa, A., Sakurai, M., Aoki, S., Uchida, K., and Wada, K. (2008) *Hum. Mol. Genet.* **17,** 1482–1496
14. Lowe, J., McDermott, H., Landon, M., Mayer, R. J., and Wilkinson, K. D. (1990) *J. Pathol.* **161,** 153–160
15. Maraganore, D. M., Lesnick, T. G., Elbaz, A., Chartier-Harlin, M. C., Gasser, T., Kruger, R., Hattori, N., Mellick, G. D., Quattrone, A., Satoh, J., Toda, T., Wang, J., Ioannidis, J. P., de Andrade, M., and Rocca, W. A. (2004) *Ann. Neurol.* **55,** 512–521
16. Healy, D. G., Abou-Sleiman, P. M., Casas, J. P., Ahmadi, K. R., Lynch, T., Gandhi, S., Muqit, M. M., Foltynie, T., Barker, R., Bhatia, K. P., Quinn, N. P., Lees, A. J., Gibson, J. M., Holton, J. L., Revesz, T., Goldstein, D. B., and Wood, N. W. (2006) *Ann. Neurol.* **59,** 627–633
17. Choi, J., Levey, A. I., Weintraub, S. T., Rees, H. D., Gearing, M., Chin, L. S., and Li, L. (2004) *J. Biol. Chem.* **279,** 13256–13264
18. Wilkinson, K. D., Lee, K. M., Deshpande, S., Duerksen-Hughes, P., Boss, J. M., and Pohl, J. (1989) *Science* **246,** 670–673
19. Larsen, C. N., Krantz, B. A., and Wilkinson, K. D. (1998) *Biochemistry* **37,** 3358–3368
20. Liu, Y., Fallon, L., Lashuel, H. A., Liu, Z., and Lansbury, P. T., Jr. (2002) *Cell* **111,** 209–218
21. Osaka, H., Wang, Y. L., Takada, K., Takizawa, S., Setsuie, R., Li, H., Sato, Y., Nishikawa, K., Sun, Y. J., Sakurai, M., Harada, T., Hara, Y., Kimura, I., Chiba, S., Namikawa, K., Kiyama, H., Noda, M., Aoki, S., and Wada, K. (2003) *Hum. Mol. Genet.* **12,** 1945–1958
22. Nishikawa, K., Li, H., Kawamura, R., Osaka, H., Wang, Y. L., Hara, Y., Hirokawa, T., Manago, Y., Amano, T., Noda, M., Aoki, S., and Wada, K. (2003) *Biochem. Biophys. Res. Commun.* **304,** 176–183
23. Saigoh, K., Wang, Y. L., Suh, J. G., Yamanishi, T., Sakai, Y., Kiyosawa, H., Harada, T., Ichihara, N., Wakana, S., Kikuchi, T., and Wada, K. (1999) *Nat. Genet.* **23,** 47–51
24. Cuervo, A. M., Stefanis, L., Fredenburg, R., Lansbury, P. T., and Sulzer, D. (2004) *Science* **305,** 1292–1295
25. Cuervo, A. M. (2004) *Trends Cell Biol.* **14,** 70–77
26. Agarraberes, F. A., and Dice, J. F. (2001) *J. Cell Sci.* **114,** 2491–2499
27. Finn, P. F., and Dice, J. F. (2005) *J. Biol. Chem.* **280,** 25864–25870
28. Kabuta, T., Suzuki, Y., and Wada, K. (2006) *J. Biol. Chem.* **281,** 30524–30533
29. Pertoft, H., Warmegard, B., and Hook, M. (1978) *Biochem. J.* **174,** 309–317
30. Kabuta, T., Hakuno, F., Asano, T., and Takahashi, S. (2002) *J. Biol. Chem.* **277,** 6846–6851
31. Eskelinen, E. L., Cuervo, A. M., Taylor, M. R., Nishino, I., Blum, J. S., Dice, J. F., Sandoval, I. V., Lippincott-Schwartz, J., August, J. T., and Saftig, P. (2005) *Traffic* **6,** 1058–1061
32. Dice, J. F. (1990) *Trends Biochem. Sci.* **15,** 305–309
33. Levine, B., and Kroemer, G. (2008) *Cell* **132,** 27–42
34. Webb, J. L., Ravikumar, B., Atkins, J., Skepper, J. N., and Rubinsztein, D. C. (2003) *J. Biol. Chem.* **278,** 25009–25013
35. Das, C., Hoang, Q. Q., Kreinbring, C. A., Luchansky, S. J., Meray, R. K., Ray, S. S., Lansbury, P. T., Ringe, D., and Petsko, G. A. (2006) *Proc. Natl. Acad.*

Sci. U. S. A. **103,** 4675–4680
36. Majeski, A. E., and Dice, J. F. (2004) *Int. J. Biochem. Cell Biol.* **36,** 2435–2444
37. Baba, M., Nakajo, S., Tu, P. H., Tomita, T., Nakaya, K., Lee, V. M., Trojanowski, J. Q., and Iwatsubo, T. (1998) *Am. J. Pathol.* **152,** 879–884
38. Johnston, S. C., Riddle, S. M., Cohen, R. E., and Hill, C. P. (1999) *EMBO J.* **18,** 3877–3887
39. Ischiropoulos, H., and Beckman, J. S. (2003) *J. Clin. Investig.* **111,** 163–169
40. Naito, S., Mochizuki, H., Yasuda, T., Mizuno, Y., Furusaka, M., Ikeda, S., Adachi, T., Shimizu, H. M., Suzuki, J., Fujiwara, S., Okada, T., Nishikawa, K., Aoki, S., and Wada, K. (2006) *Biochem. Biophys. Res. Commun.* **339,** 717–725
41. Solano, S. M., Miller, D. W., Augood, S. J., Young, A. B., and Penney, J. B., Jr. (2000) *Ann. Neurol.* **47,** 201–210

[Autophagy 4:6, 1-3; 16 August 2008]; ©2008 Landes Bioscience

Article Addendum

Insights into links between familial and sporadic Parkinson's disease

Physical relationship between UCH-L1 variants and chaperone-mediated autophagy

Tomohiro Kabuta and Keiji Wada

Department of Degenerative Neurological Diseases; National Institute of Neuroscience; National Center of Neurology and Psychiatry; Kodaira, Tokyo, Japan

Abbreviations: UCH-L1, ubiquitin C-terminal hydrolase L1; PD, Parkinson's disease; CMA, chaperone-mediated autophagy; WT, wild-type; LAMP-2, lysosome-associated membrane protein type 2; Hsc70, heat shock cognate protein 70; Hsp90, heat shock protein 90; GAPDH, glyceraldehyde-3-phosphate dehydrogenase; HAE, 4-hydroxy-2-alkenals; HNE, 4-hydroxy-2-nonenal

Key words: ubiquitin C-terminal hydrolase L1 (UCH-L1), Parkinson's disease, LAMP-2, chaperone-mediated autophagy, α-synuclein

Ubiquitin C-terminal hydrolase L1 (UCH-L1) is expressed abundantly in neurons and has been reported to be a major target of oxidative/carbonyl damage associated with sporadic Parkinson's disease (PD). The I93M mutation in UCH-L1 is also associated with familial PD. We recently reported that UCH-L1 physically interacts with LAMP-2A, the lysosomal receptor for chaperone-mediated autophagy (CMA), and Hsc70 and Hsp90, both of which can function as components of the CMA pathway. We found that the levels of these interactions were aberrantly increased by the I93M mutation, and that expression of I93M UCH-L1 in cells induced the CMA inhibition-associated increase in the amount of α-synuclein, a risk factor for PD. The interactions of UCH-L1 with LAMP-2A, Hsc70 and Hsp90 were also abnormally enhanced by carbonyl modification of UCH-L1. We propose that aberrant interactions of UCH-L1 variants with CMA machinery, at least partly, underlie the pathogenesis of I93M UCH-L1-associated PD, and possibly of sporadic PD. Our findings may provide novel insights into the links between familial and sporadic PD.

Parkinson's disease (PD) is the most common neurodegenerative movement disorder. It is characterized by progressive cell loss of dopaminergic neurons in the substantia nigra pars compacta. A missense mutation in the ubiquitin C-terminal hydrolase L1 (UCH-L1) gene, leading to an I93M substitution at the amino acid residue level, has been reported in a German family with dominantly inherited PD.[1] We have previously shown that I93M UCH-L1-transgenic mice exhibit progressive cell loss of dopaminergic neurons.[2] Compared with wild-type (WT) UCH-L1, I93M UCH-L1 displays increased insolubility and levels of interactions with other proteins in mammalian cells, features that are characteristic of several neurodegenerative disease-linked mutants.[3] These findings suggest that the I93M mutation in UCH-L1 is a causative mutation for PD. Although the binding of I93M UCH-L1 to monoubiquitin as well as the hydrolase activity of I93M UCH-L1 are decreased compared with those of WT UCH-L1,[1,3,4] mice deficient in UCH-L1 do not display obvious dopaminergic cell loss.[5,6] Thus, the main cause of I93M UCH-L1-associated PD may not be a loss of UCH-L1 function but an acquired toxicity of I93M UCH-L1. Our previous studies suggest that aberrantly enhanced physical interactions between I93M UCH-L1 and multiple proteins, including tubulin, underlie the toxic functions of I93M UCH-L1 (Fig. 1).[3]

Several missense mutations in the α-synuclein gene are also linked to dominant-inherited PD.[7-9] α-Synuclein is thought to be a major component of cytoplasmic inclusions called Lewy bodies in the brains of patients with sporadic PD.[10,11] Increases in the levels of α-synuclein could constitute a cause of PD, since duplication and triplication of the α-synuclein gene cause familial PD or parkinsonism.[12-14] α-Synuclein is degraded at least partly by chaperone-mediated autophagy (CMA).[15]

To elucidate the molecular relationship between α-synuclein and UCH-L1 in the pathogenesis of PD, we sought to identify novel UCH-L1-interacting proteins. We found that UCH-L1 interacts with lysosome-associated membrane protein type 2A (LAMP-2A), heat shock cognate protein 70 (Hsc70) and heat shock protein 90 (Hsp90),[16] all of which are components of the CMA pathway.[17] These interactions were enhanced by the I93M mutation in UCH-L1.[16] Expression of I93M UCH-L1 in cells induced the increase in the amount of α-synuclein and glyceraldehyde-3-phosphate dehydrogenase (GAPDH),[16] both of which are substrates of CMA,[15] but had almost no effects on the amount of ΔDQ α-synuclein,[16] which lacks the CMA recognition motif.[15] Based on these results, we propose that the aberrant interaction of I93M UCH-L1 with CMA machinery causes the accumulation of α-synuclein and GAPDH by inhibiting CMA. Besides its role in glycolysis, GAPDH is known to initiate a cell-death cascade.[18] Thus, it is possible that the increases in

Correspondence to: Tomohiro Kabuta or Keiji Wada; Department of Degenerative Neurological Diseases; National Institute of Neuroscience; National Center of Neurology and Psychiatry; 4-1-1 Ogawahigashi; Kodaira, Tokyo 187-8502 Japan; Tel.: +81.42.346.1715; Fax: +81.42.346.1745; Email: kabuta@ncnp.go.jp or wada@ncnp.go.jp

Submitted: 07/03/08; Revised: 07/08/08; Accepted: 07/08/08

Previously published online as an *Autophagy* Epublication: www.landesbioscience.com/journals/autophagy/article/6560

Addendum to: Kabuta T, Furuta A, Aoki S, Furuta K, Wada K. Aberrant interaction between Parkinson disease-associated mutant UCH-L1 and the lysosomal receptor for chaperone-mediated autophagy. J Biol Chem 2008; Epub ahead of print.

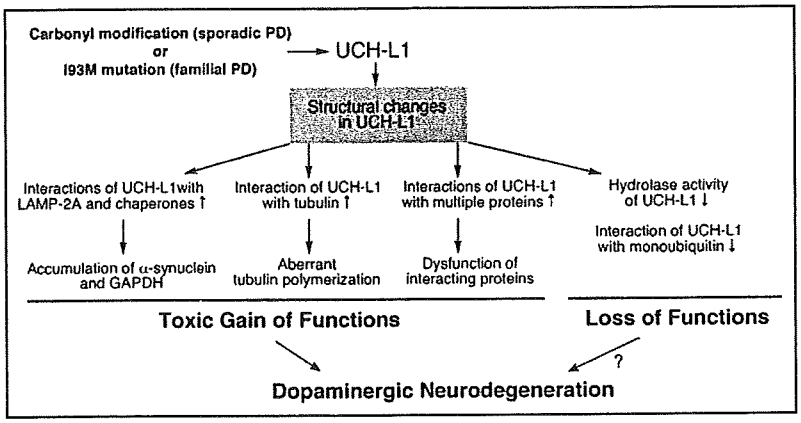

Figure 1. Possible role of UCH-L1 in PD. The I93M mutation (as occurs in familial PD associated with I93M UCH-L1) and carbonyl-modification (as occurs in sporadic PD) cause structural changes in UCH-L1. The hydrolase activity and binding affinity to monoubiquitin of these UCH-L1 proteins are decreased. The involvement of loss of UCH-L1 functions in the pathogenesis of PD is currently unclear. Abnormal UCH-L1 interacts tightly with LAMP-2A, Hsc70 and Hsp90. These abnormal UCH-L1 may inhibit CMA-dependent degradation, and cause CMA substrates including α-synuclein and GAPDH to accumulate. The increased amount of α-synuclein or GAPDH proteins possibly contributes to the neurodegeneration of dopaminergic neurons. The aberrant interactions of UCH-L1 with other proteins, including tubulin, may also contribute to neurodegeneration. ↑: increase compared with wild-type UCH-L1, ↓: decrease compared with wild-type UCH-L1.

the amount of α-synuclein and GAPDH are involved in the pathogenesis of PD (Fig. 1).

Although the majority of PD cases occur sporadically, the molecular mechanisms that underlie the pathology of sporadic PD are poorly understood. It is known that oxidative/carbonyl stresses are elevated in PD brains.[19,20] In the brains of sporadic PD patients, UCH-L1 is a major target of carbonyl formation,[19] which is the most widely used marker for oxidative damage to proteins. Carbonyl groups can be introduced into proteins in vivo mainly by reactions with 2-alkenals, 4-hydroxy-2-alkenals (HAE) or ketoaldehydes,[21,22] which are endogenous aldehyde products formed by lipid peroxidation or glycooxidation. Protein carbonyls can also be produced by metal-catalyzed reactions with H_2O_2 in vitro.[22,23] It has been suggested that 4-hydroxy-2-nonenal (HNE) can accumulate in biological membranes at concentrations of over 10–100 μM in response to oxidative stress.[24,25] In mammalian cells, carbonyl-modified UCH-L1 can be produced by reactions with 10–100 μM HAE or 2-alkenals, but not by 100–500 μM ketoaldehydes or 0.1–1 mM H_2O_2.[3] Furthermore, I93M UCH-L1 and carbonyl-modified UCH-L1 display shared aberrant properties,[3] suggesting that carbonyl-modified UCH-L1 constitutes one of the causes of sporadic PD. Therefore, we tested the effects of carbonyl modification of UCH-L1 on the interaction of UCH-L1 with LAMP-2A and chaperones. We found that HNE modification of UCH-L1 promotes interactions between UCH-L1 and LAMP-2A, Hsc70 or Hsp90 (Fig. 2A). 4-hydroxy-2-hexenal or 2-propenal modification of UCH-L1 have similar effects on the interactions between UCH-L1 and LAMP-2A, Hsc70 or Hsp90 as HNE modification (data not shown). In a pull-down assay, HNE-modified UCH-L1 exhibits an abnormally increased level of interaction with the cytosolic region of LAMP-2A, compared with wild-type UCH-L1 (data not shown). Thus, I93M UCH-L1 and carbonyl-modified UCH-L1 also exhibit common biochemical properties with respect to their interactions with LAMP-2A, Hsc70 and Hsp90. These results support the idea that carbonyl-modified UCH-L1 constitutes one of the causes of sporadic PD (Fig. 1). A coimmunoprecipitation assay using C90S, C132S and C152S UCH-L1 mutants shows less binding of C90S UCH-L1 to LAMP-2A, Hsc70 or Hsp90 than WT UCH-L1, when cells are treated with HNE (Fig. 2B and C). Thus, HNE modification of Cys-90 of UCH-L1 promotes the interactions of UCH-L1 with LAMP-2A, Hsc70 and Hsp90. These results are consistent with our previous data showing that the HAE modification of Cys-90 of UCH-L1 promotes the interactions of UCH-L1 with multiple proteins.[3]

The appearance of HNE-modified proteins in nigral neurons is associated with sporadic PD.[26,27] We have previously observed that cysteine residues in UCH-L1 are main targets for HNE-modification of UCH-L1.[3] UCH-L1 is modified by 10–100 μM HNE, whereas α-synuclein, which contains no cysteine residues, is not modified by 100 μM HNE in mammalian cells,[3] suggesting that, in mammalian cells, HNE reacts with proteins mainly via cysteine residues. It is possible that, in sporadic PD, cysteine residue-reactive carbonyl stresses such as HAE result in the accumulation of α-synuclein, not by direct modification of α-synuclein, but via reaction with UCH-L1.

In conclusion, aberrant interactions of UCH-L1 variants with multiple proteins, including CMA machinery, may underlie the pathogenesis of I93M UCH-L1-associated PD, and possibly of sporadic PD. We propose that carbonyl modification of UCH-L1 can be a therapeutic target for the treatment of sporadic PD.

References

1. Leroy E, Boyer R, Auburger G, Leube B, Ulm G, Mezey E, Harta G, Brownstein MJ, Jonnalagada S, Chernova T, Dehejia A, Lavedan C, Gasser T, Steinbach PJ, Wilkinson KD, Polymeropoulos MH. The ubiquitin pathway in Parkinson's disease. Nature 1998; 395:451-2.
2. Setsuie R, Wang YL, Mochizuki H, Osaka H, Hayakawa H, Ichihara N, Li H, Furuta A, Sano Y, Sun YJ, Kwon J, Kabuta T, Yoshimi K, Aoki S, Mizuno Y, Noda M, Wada K. Dopaminergic neuronal loss in transgenic mice expressing the Parkinson's disease-associated UCH-L1 I93M mutant. Neurochem Int 2007; 50:119-29.
3. Kabuta T, Setsuie R, Mitsui T, Kinugawa A, Sakurai M, Aoki S, Uchida K, Wada K. Aberrant molecular properties shared by familial Parkinson's disease-associated mutant UCH-L1 and carbonyl-modified UCH-L1. Hum Mol Genet 2008; 17:1482-96.
4. Nishikawa K, Li H, Kawamura R, Osaka H, Wang YL, Hara Y, Hirokawa T, Manago Y, Amano T, Noda M, Aoki S, Wada K. Alterations of structure and hydrolase activity of parkinsonism-associated human ubiquitin carboxyl-terminal hydrolase L1 variants. Biochem Biophys Res Commun 2003; 304:176-83.
5. Saigoh K, Wang YL, Suh JG, Yamanishi T, Sakai Y, Kiyosawa H, Harada T, Ichihara N, Wakana S, Kikuchi T, Wada K. Intragenic deletion in the gene encoding ubiquitin carboxy-terminal hydrolase in gad mice. Nat Genet 1999; 23:47-51.
6. Osaka H, Wang YL, Takada K, Takizawa S, Setsuie R, Li H, Sato Y, Nishikawa K, Sun YJ, Sakurai M, Harada T, Hara Y, Kimura I, Chiba S, Namikawa K, Kiyama H, Noda M, Aoki S, Wada K. Ubiquitin carboxy-terminal hydrolase L1 binds to and stabilizes monoubiquitin in neuron. Hum Mol Genet 2003; 12:1945-58.
7. Polymeropoulos MH, Lavedan C, Leroy E, Ide SE, Dehejia A, Dutra A, Pike B, Root H, Rubenstein J, Boyer R, Stenroos ES, Chandrasekharappa S, Athanassiadou A, Papapetropoulos T, Johnson WG, Lazzarini AM, Duvoisin RC, Di Iorio G, Golbe LI, Nussbaum RL. Mutation in the α-synuclein gene identified in families with Parkinson's disease. Science 1997; 276:2045-7.

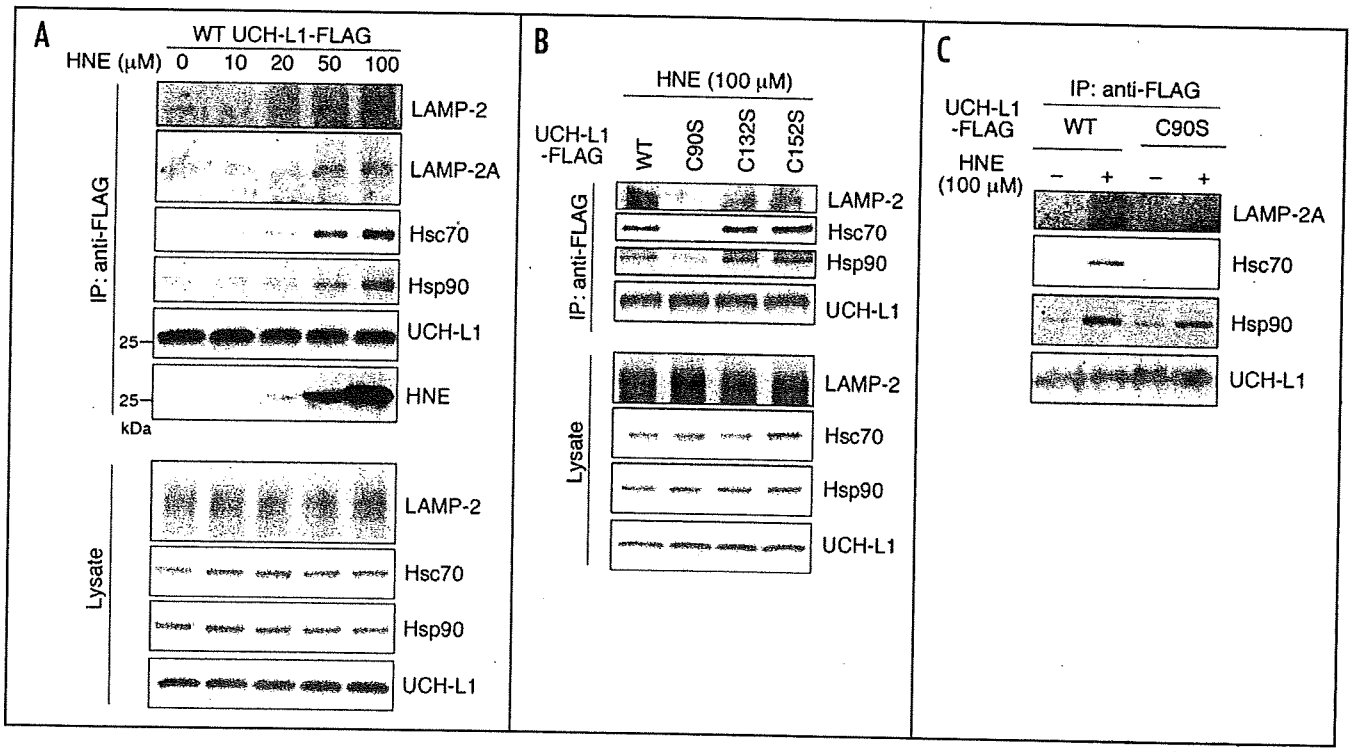

Figure 2. Effects of HNE-modification of UCH-L1 on the interactions of UCH-L1 with LAMP-2A, Hsc70 and Hsp90 (A) COS-7 cells transfected with FLAG-tagged WT UCH-L1 were treated with the indicated concentrations of HNE. Lysates were immunoprecipitated with anti-FLAG antibody, and analyzed by immunoblotting using anti-LAMP-2, LAMP-2A, Hsc70, Hsp90, HNE and FLAG antibodies. (B and C) COS-7 cells transfected with the indicated constructs were treated with or without 100 μM HNE. Lysates were immunoprecipitated using anti-FLAG antibody, and analyzed by immunoblotting.

8. Kruger R, Kuhn W, Muller T, Woitalla D, Graeber M, Kosel S, Przuntek H, Epplen JT, Schols L, Riess O. Ala30Pro mutation in the gene encoding alpha-synuclein in Parkinson's disease. Nat Genet 1998; 18:106-8.
9. Zarranz JJ, Alegre J, Gomez-Esteban JC, Lezcano E, Ros R, Ampuero I, Vidal L, Hoenicka J, Rodriguez O, Atares B, Llorens V, Gomez Tortosa E, del Ser T, Munoz DG, de Yebenes JG. The new mutation, E46K, of α-synuclein causes Parkinson and Lewy body dementia. Ann Neurol 2004; 55:164-73.
10. Spillantini MG, Schmidt ML, Lee VM, Trojanowski JQ, Jakes R, Goedert M. Alpha-synuclein in Lewy bodies. Nature 1997; 388:839-40.
11. Spillantini MG, Crowther RA, Jakes R, Hasegawa M, Goedert M. alpha-Synuclein in filamentous inclusions of Lewy bodies from Parkinson's disease and dementia with lewy bodies. Proc Natl Acad Sci USA 1998; 95:6469-73.
12. Chartier-Harlin MC, Kachergus J, Roumier C, Mouroux V, Douay X, Lincoln S, Levecque C, Larvor L, Andrieux J, Hulihan M, Waucquier N, Defebvre L, Amouyel P, Farrer M, Destee A. α-synuclein locus duplication as a cause of familial Parkinson's disease. Lancet 2004; 364:1167-9.
13. Ibanez P, Bonnet AM, Debarges B, Lohmann E, Tison F, Pollak P, Agid Y, Durr A, Brice A. Causal relation between α-synuclein gene duplication and familial Parkinson's disease. Lancet 2004; 364:1169-71.
14. Singleton AB,, Farrer M, Johnson J, Singleton A, Hague S, Kachergus J, Hulihan M, Peuralinna T, Dutra A, Nussbaum R, Lincoln S, Crawley A, Hanson M, Maraganore D, Adler C, Cookson MR, Muenter M, Baptista M, Miller D, Blancato J, Hardy J, Gwinn-Hardy K. α-Synuclein locus triplication causes Parkinson's disease. Science 2003; 302:841.
15. Cuervo AM, Stefanis L, Fredenburg R, Lansbury PT, Sulzer D. Impaired degradation of mutant α-synuclein by chaperone-mediated autophagy. Science 2004; 305:1292-5.
16. Kabuta T, Furuta A, Aoki S, Furuta K, Wada K. Aberrant interaction between Parkinson disease-associated mutant UCH-L1 and the lysosomal receptor for chaperone-mediated autophagy. J Biol Chem 2008; Epub ahead of print.
17. Agarraberes FA, Dice JF. A molecular chaperone complex at the lysosomal membrane is required for protein translocation. J Cell Sci 2001; 114:2491-9.
18. Sen N, Hara MR, Kornberg MD, Cascio MB, Bae BI, Shahani N, Thomas B, Dawson TM, Dawson VL, Snyder SH, Sawa A. Nitric oxide-induced nuclear GAPDH activates p300/CBP and mediates apoptosis. Nat Cell Biol 2008; Epub ahead of print.
19. Choi J, Levey AI, Weintraub ST, Rees HD, Gearing M, Chin LS, Li L. Oxidative modifications and down-regulation of ubiquitin carboxyl-terminal hydrolase L1 associated with idiopathic Parkinson's and Alzheimer's diseases. J Biol Chem 2004; 279:13256-64.
20. Ischiropoulos H, Beckman JS. Oxidative stress and nitration in neurodegeneration: cause, effect, or association? J Clin Invest 2003; 111:163-9.
21. Uchida K. Role of reactive aldehyde in cardiovascular diseases. Free Radic Biol Med 2000; 28:1685-96.
22. Uchida K. Histidine and lysine as targets of oxidative modification. Amino Acids 2003; 25:249-57.
23. Stadtman ER. Oxidation of free amino acids and amino acid residues in proteins by radiolysis and by metal-catalyzed reactions. Annu Rev Biochem 1993; 62:797-821.
24. Uchida K. 4-Hydroxy-2-nonenal: a product and mediator of oxidative stress. Prog Lipid Res 2003; 42:318-43.
25. Esterbauer H, Schaur RJ, Zollner H. Chemistry and biochemistry of 4-hydroxynonenal, malonaldehyde and related aldehydes. Free Radic Biol Med 1991; 11:81-128.
26. Yoritaka A, Hattori N, Uchida K, Tanaka M, Stadtman ER, Mizuno Y. Immunohistochemical detection of 4-hydroxynonenal protein adducts in Parkinson disease. Proc Natl Acad Sci USA 1996; 93:2696-701.
27. Castellani RJ, Perry G, Siedlak SL, Nunomura A, Shimohama S, Zhang J, Montine T, Sayre LM, Smith MA. Hydroxynonenal adducts indicate a role for lipid peroxidation in neocortical and brainstem Lewy bodies in humans. Neurosci Lett 2002; 319:25-8.

Journal of Neurochemistry JNC

JOURNAL OF NEUROCHEMISTRY | 2009 | 108 | 932–944 doi: 10.1111/j.1471-4159.2008.05827.x

Effects of UCH-L1 on α-synuclein over-expression mouse model of Parkinson's disease

Toru Yasuda,* Tomoko Nihira,* Yong-Ri Ren,* Xu-Qing Cao,† Keiichiro Wada,† Rieko Setsuie,‡ Tomohiro Kabuta,‡ Keiji Wada,‡ Nobutaka Hattori,† Yoshikuni Mizuno* and Hideki Mochizuki*,†

*Research Institute for Diseases of Old Age, Juntendo University, Tokyo, Japan

†Department of Neurology, Juntendo University School of Medicine, Tokyo, Japan

‡Department of Degenerative Neurological Diseases, National Institute of Neuroscience, National Center of Neurology and Psychiatry, Tokyo, Japan

Abstract

The rare inherited form of Parkinson's disease (PD), *PARK5*, is caused by a missense mutation in *ubiquitin carboxy-terminal hydrolase-L1* (*UCH-L1*) gene, resulting in Ile93Met substitution in its gene product (UCH-L1^{Ile93Met}). *PARK5* is inherited in an autosomal-dominant mode, but whether the Ile93Met mutation gives rise to a gain-of-toxic-function or loss-of-function of UCH-L1 protein remains controversial. Here, we investigated the selective vulnerabilities of dopaminergic (DA) neurons in UCH-L1-transgenic (Tg) and spontaneous UCH-L1-null *gracile axonal dystrophy* mice to an important PD-causing insult, abnormal accumulation of α-synuclein (αSyn). Immunohistochemistry of midbrain sections of a patient with sporadic PD showed αSyn- and UCH-L1-double-positive Lewy bodies in nigral DA neurons, suggesting physical and/or functional interaction between the two proteins in human PD brain. Recombinant adeno-associated viral vector-mediated over-expression of αSyn for 4 weeks significantly enhanced the loss of nigral DA cell bodies in UCH-L1^{Ile93Met}-Tg mice, but had weak effects in age-matched UCH-L1$^{wild\text{-}type}$-Tg mice and non-Tg littermates. In contrast, the extent of αSyn-induced DA cell loss in *gracile axonal dystrophy* mice was not significantly different from wild-type littermates at 13-weeks post-injection. Our results support the hypothesis that *PARK5* is caused by a gain-of-toxic-function of UCH-L1^{Ile93Met} mutant, and suggest that regulation of UCH-L1 in nigral DA cells could be a future target for treatment of PD.

Keywords: α-synuclein, adeno-associated virus, dopaminergic neurons, Parkinson's disease, ubiquitin carboxy-terminal hydrolase-L1.

J. Neurochem. (2009) **108**, 932–944.

Parkinson's disease (PD) is a progressive neurodegenerative disorder characterized clinically by resting tremor, rigidity, akinesia, and postural instability (Farrer 2006). The major pathological hallmarks of PD are the selective loss of nigrostriatal dopaminergic (DA) neurons and the presence of intraneuronal protein inclusions termed Lewy bodies, in the surviving DA neurons. Sporadic cases represent more than 90% of total patients with PD, while there exist several inherited forms (familial PD; fPD) caused by mutations in single genes. Identification and characterization of these causative genes and their products can help us understand the molecular mechanism(s) of DA neurodegeneration in the sporadic form of PD. Seven causative genes for fPDs have been identified to date; those encoding α-synuclein (αSyn), parkin, UCH-L1, PINK1, DJ-1, LRRK2, or ATP13A2 (Farrer 2006; Ramirez *et al.* 2006).

α-Synuclein is a pre-synaptic protein potentially involved in learning, synaptic plasticity, vesicle dynamics, and dopamine synthesis (Farrer 2006). The fPD *PARK1* is caused by

Received August 26, 2008; revised manuscript received November 6, 2008; accepted November 27, 2008.

Address correspondence and reprint requests to Hideki Mochizuki, Department of Neurology, Juntendo University School of Medicine, 2-1-1 Hongo, Bunkyo-ku, Tokyo, 113-8421, Japan.
E-mail: hideki@med.juntendo.ac.jp

Abbreviations used: αSyn, α-synuclein; DA, dopaminergic; DOPAC, 2-(3,4-dihydroxyphenyl)acetic acid; fPD, familial Parkinson's disease; *gad, gracile axonal dystrophy*; hrGFP, humanized recombinant green fluorescent protein; HVA, homovanillic acid; PBS, phosphate-buffered saline; PD, Parkinson's disease; rAAV, recombinant adeno-associated virus; SN, substantia nigra; SNpc, substantia nigra pars compacta; Tg, transgenic; TH, tyrosine hydroxylase; UCH-L1, ubiquitin carboxy-terminal hydrolase-L1.

missense mutations resulting in amino acid substitutions in αSyn protein (Ala53Thr, Ala30Pro, or Glu46Lys) (Polymeropoulos *et al.* 1997; Kruger *et al.* 1998; Zarranz *et al.* 2004). Furthermore, *PARK4* is caused by duplication or triplication of *αSyn* gene (*SNCA*) locus (Singleton *et al.* 2003; Nishioka *et al.* 2006). In sporadic cases of PD, αSyn protein is the major component of Lewy bodies (Spillantini *et al.* 1997; Baba *et al.* 1998). These findings suggest an important role for αSyn protein accumulation in DA cells in the pathogenesis of PD. Previous studies also reported that over-expression of αSyn protein by using a recombinant adeno-associated viral (rAAV) or lentiviral vector caused DA neurodegeneration in rats and monkeys (Kirik *et al.* 2002, 2003; Lo Bianco *et al.* 2002; Yamada *et al.* 2004; Yasuda *et al.* 2007).

Ubiquitin carboxy-terminal hydrolase-L1 constitutes 1–2% of brain proteins and functions in the ubiquitin-proteasome system (Wilkinson *et al.* 1989; Larsen *et al.* 1996, 1998). The ubiquitin hydrolase activity of UCH-L1 is important to free reusable ubiquitin monomers. UCH-L1 protein is also known to bind to and stabilize monomeric ubiquitin molecule (Osaka *et al.* 2003). *PARK5* is caused by a missense mutation in *UCH-L1* gene resulting in Ile93Met substitution in UCH-L1 protein (UCH-L1^{Ile93Met}), and inherited in an autosomal-dominant mode (Leroy *et al.* 1998). The UCH-L1^{Ile93Met} mutant was initially shown to have decreased ubiquitin hydrolase activity (Leroy *et al.* 1998; Nishikawa *et al.* 2003). In sporadic PD cases, wild-type UCH-L1 protein is deposited in Lewy bodies (Lowe *et al.* 1990). These controversial findings initiated a debate on whether the Ile93Met mutation results in gain-of-toxic-function or loss-of-function of UCH-L1 protein. Recently, we established transgenic (Tg) mice that over-express UCH-L1^{Ile93Met} protein of human origin (Setsuie *et al.* 2007). These mice showed behavioral and pathological phenotypes of Parkinsonism at 20 weeks of age (Setsuie *et al.* 2007). On the other hand, the *gracile axonal dystrophy* (*gad*) mouse, which exhibits age-dependent sensory ataxic phenotype and motor paresis, has spontaneous intragenic deletion of mouse *Uchl1* gene and systemic lack of the UCH-L1 protein expression (Saigoh *et al.* 1999). The pathological characteristics of these mice are 'dying-back' axonal degeneration in sensory and motor nerve terminals (Oda *et al.* 1992; Miura *et al.* 1993). However, they do not seem to show any pathological changes in the nigrostriatal DA pathway, especially the loss of DA cell bodies in the substantia nigra (SN). To our knowledge, no investigator has examined the vulnerability of DA neurons in *gad* mice to PD-causing insults.

The aim of the present study was to determine the functional interaction between αSyn and UCH-L1 proteins *in vivo*. Specifically, we examined whether the DA neurotoxicity associated with accumulation of αSyn protein is influenced by UCH-L1 mutation or absence of normal UCH-L1 activities. Identification of such interaction could be useful in the design of novel gene therapies that target UCH-L1.

Materials and methods

Human brain tissue

Autopsied brain of a 69-year-old female PD patient was used in this study. The diagnosis of PD was confirmed at the Department of Neurology, Juntendo University School of Medicine. The study protocol was approved by the Human Ethics Review Committee of Juntendo University School of Medicine. The autopsied midbrain tissue was cut into blocks, immediately fixed in phosphate-buffered 4% formaldehyde for 2 days. Then the tissue blocks were immersed in phosphate-buffered saline (PBS) containing 30% sucrose until sinking. Coronal sections were cut at a thickness of 30 μm using a freezing microtome.

Mice

The Tg mice lines of UCH-L1^{Ile93Met} (line H-hI93M) and UCH-L1$^{wild\text{-}type}$ (line hWT) were generated as described previously using fertilized eggs of C57BL/6 mice (Setsuie *et al.* 2007). Male UCH-L1^{Ile93Met}-Tg mice were bred with female C57BL/6 mice (Charles River Laboratories, Kanagawa, Japan), to obtain Tg and non-Tg littermates. The latter were used in the experiment at the ages of 13 weeks (denoted as 3-month-old) and 52–57 weeks (12-month-old). Male UCH-L1$^{wild\text{-}type}$-Tg mice were bred with female C57BL/6 mice, and the obtained Tg mice were used in the experiment at the ages of 13 weeks (3-month-old) and 53–57 weeks (12-month-old). At 3 and 12 months of age, the number of DA cells in UCH-L1^{Ile93Met}-Tg mice was not significantly different from those of age-matched non-Tg littermates (Setsuie *et al.* 2007; and this study, data not shown). Male and female mice heterozygous for *gad* allele were bred, and the obtained *gad* and wild-type littermates were used in the experiments at the age of 13 weeks (3-month-old). The *gad* mice line had been backcrossed to C57BL/6 background for at least 15 generations. The experimental protocol was approved by the Ethics Review Committee for Animal Experimentation of Juntendo University School of Medicine, and all surgical operations were performed according to rules set forth by the Ethics Committee for the Use of Laboratory Animals at Juntendo University.

Preparation of rAAV vector

The plasmid pAAV-MCS (CMV promoter; Stratagene, La Jolla, CA, USA) carrying human *αSyn* cDNA (pAAV-MCS-αSyn) was constructed as reported previously (Yamada *et al.* 2004). High-titer serotype-1 rAAV (rAAV1) vector stocks were prepared as described previously (Yasuda *et al.* 2007). In brief, the plasmid pAAV-MCS-αSyn or pAAV-hrGFP (humanized recombinant green fluorescent protein; Stratagene) was co-transfected with plasmids pHelper and Pack2/1 (kindly provided by Dr. T. Shimada, Nippon Medical School, Tokyo, Japan) to HEK293 cells using a standard calcium phosphate method (Sambrook and Russell 2001). After 48 h, the cells were harvested and the crude rAAV1 vector solutions were obtained by repeated freeze/thaw cycles. After ammonium sulfate precipitation, the virus particles were dissolved in PBS and applied to OptiSeal centrifugation tube (Beckman Coulter, Inc., Fullerton,

CA, USA). After overlaying the OptiPrep solution (Axis-Shield PoC AS, Oslo, Norway), the tube was processed by GradientMaster (BioComp Instruments, Inc., New Brunswick, Canada) to prepare a gradient layer of OptiPrep. The tube was then ultracentrifuged at 20 000 *g* for 18.5 h. The fractions containing high-titer rAAV1 vectors were collected and used for the injection into mice. The number of rAAV1 genome copies was quantified by PCR within the CMV promoter region using primers 5′-GACGTCAATAATGACG-TATG-3′ and 5′-GGTAATAGCGATGACTAATACG-3′. The titer of rAAV1 vector to produce human αSyn (designated rAAV1-αSyn) was 6×10^{11} genomes/mL, and the titer of rAAV1 vector to produce hrGFP (rAAV1-hrGFP) was 6×10^{11} genomes/mL.

Stereotaxic injection of rAAV1 vectors

Mice were anesthetized with sodium pentobarbital (50 mg/kg body weight; intraperitoneally, i.p.) and positioned in a stereotaxic frame. The skull was exposed, and a small portion of the skull over the SN was removed unilaterally with a dental drill. Subsequently, rAAV1-αSyn or rAAV1-hrGFP was injected unilaterally into the SN (2 μL, 2.8 mm posterior and 1.3 mm lateral from the bregma, 4.4 mm below the dural surface, tooth bar = −2 mm) through a 5-μL Hamilton microsyringe.

The rAAV1-injected UCH-L1$^{\text{wild-type}}$-Tg, UCH-L1$^{\text{Ile93Met}}$-Tg mice, and non-Tg littermates were killed at 4-weeks post-injection, while the rAAV1-injected *gad* and wild-type littermates were killed at 4-, 8-, or 13-weeks post-injection. Mice were deeply anesthetized with sodium pentobarbital (250 mg/kg body weight; i.p.) and perfused transcardially with PBS. The brains were removed *en bloc* from the skull, and cut coronally along the anterior tangent to the median eminence. The striatal tissues were then dissected and immediately frozen on dry ice. The posterior parts of brain blocks including the entire rostrocaudal extent of the SN were fixed overnight in 4% paraformaldehyde in PBS, and immersed in PBS containing 30% sucrose until sinking. Coronal sections of the SN were cut serially at 20 μm thickness by a freezing microtome.

Antibodies and immunohistochemistry

The primary antibodies used in this study were as follows; mouse anti-human αSyn (clone LB509; diluted at 1 : 100; Zymed Laboratories Inc., South San Francisco, CA, USA), rabbit anti-UCH-L1 (1 : 1000; Ultraclone, Isle of Wight, UK), rabbit anti-hrGFP (1 : 500; Stratagene), sheep anti-tyrosine hydroxylase (TH) (1 : 5000; Calbiochem, San Diego, CA, USA), rabbit anti-dopamine transporter (DAT) (1 : 200; Chemicon International Inc., Temecula, CA, USA), and rabbit anti-active caspase-3 (1 : 500; BD Biosciences, San Jose, CA, USA) antibodies. The free-floating coronal sections of the human and mice brains were washed in a PBS medium containing 0.05% Triton X-100 (PBS-T), soaked with 10% Block Ace (Yukijirushi-Nyugyo Co., Sapporo, Japan) in PBS-T, and then incubated with the primary antibody dissolved in PBS-T containing 2% Block Ace at 4°C for 24–48 h. Subsequently, for fluorescent visualization of the antigens, the sections were incubated for 2 h in the same fresh medium containing the following secondary antibodies. For human brain sections, FITC-conjugated anti-mouse IgG and Cy3-conjugated anti-rabbit IgG antibodies (1 : 500; Jackson ImmunoResearch Laboratories, Inc., West Grove, PA, USA) were used. For mouse brain sections, FITC-conjugated anti-mouse IgG or anti-rabbit IgG antibody (1 : 500; Jackson ImmunoResearch Laboratories, Inc.) and Cy3-conjugated anti-sheep IgG antibody (1 : 500; Jackson ImmunoResearch Laboratories, Inc.) were used. Sections on the slides were mounted using Vectashield Mounting Medium with 4′,6-diamidino-2-phenylindole (DAPI) (Vector Laboratories Inc., Burlingame, CA, USA). Images were captured using a confocal laser-scanning microscope (LSM510, Zeiss, Jena, Germany). For colorimetric visualization of the antigen, the sections were incubated for 2 h in the same fresh medium containing biotinylated secondary antibody (anti-mouse, anti-rabbit, or anti-sheep IgG antibody; 1 : 500; Vector Laboratories Inc.), followed by avidin-biotin-peroxidase complex (ABC Elite; Vector Laboratories Inc.) for another 1 h. Then the sections were reacted in 0.05 M Tris-HCl buffer (pH 7.6) containing 0.04% diaminobenzidine and 0.002% hydrogen peroxide with (dark brown/purple color) or without (brown color) 0.04% nickel chloride. Images were captured using a light microscope (ACT-1, Nikon Corp., Tokyo, Japan).

Densitometric analysis of αSyn

The density of human αSyn-positive cells was quantified using the NIH Image software (National Institute of Mental Health, Bethesda, MD, USA). Every fourth 20-μm-thick serial section of the brain was immunostained for human αSyn and 10 single cells in the substantia nigra pars compacta (SNpc) randomly selected per section (4–7 sections per mice) were used for densitometric analysis (four mice per group). The two-tailed Student's *t*-test was applied to evaluate the statistical significance of the difference between groups. A p value less than 0.05 denoted the presence of statistically significant difference.

DA cell counting, measurement of striatal dopamine, 2-(3,4-dihydroxyphenyl)acetic acid (DOPAC), and homovanillic acid (HVA)

At first, every eighth 20-μm-thick serial sections of the brain were immunostained for hrGFP (for mice injected with rAAV1-hrGFP) or human αSyn (for mice injected with rAAV1-αSyn). Mice that exhibited foreign protein expression in DA cells in more than half area of the entire rostrocaudal region of the SNpc were used for the following investigations. The rostrocaudal area of the SNpc immunopositive for foreign protein was determined in each mouse and used for DA cell counting (see Table 1). In every fourth serial section, the numbers of TH- and Nissl-positive cells in the SNpc were counted both in the rAAV1-injected and intact sides, as reported previously (Mandir *et al.* 1999; Furuya *et al.* 2004). In brief, SNpc cells with nuclei optimally visible by TH immunostaining, and with nuclei, cytoplasm, and nucleoli prominently stained by Nissl staining were counted. The cell number was counted by an experimenter blinded to the genotypes of mice and rAAV1 groups. The data were expressed as percentage of the contralateral side; i.e., the cell number in the rAAV1-injected side over that in the intact side.

Frozen striatal tissues were sonicated in chilled 0.1 M perchloric acid. The samples were centrifuged (20 000 *g* for 10 min at 4°C) and the resulting supernatants were used for the measurement of dopamine, DOPAC, and HVA concentrations. The HPLC system equipped with a reverse-phase C18 column (150 × 4.6 mm; ODS-100s, Tosoh, Tokyo, Japan) and an eight-electrode coulometric electrochemical detection system (ESA-400, ESA. Inc., Chelmsford, MA, USA) was used. The concentrations of dopamine, DOPAC, and HVA were determined in nanomoles per gram of tissue weight. The data were expressed as percentage of contralateral side; that is, the

Table 1 Number of mice used in the present experiments and transduction efficiencies of rAAV1 vector

Mice, rAAV1	3-month-old, 4-week post-injection		12-month-old, 4-week post-injection	
	Number of mice[a]	Efficiency[b] (%)	Number of mice	Efficiency (%)
Wt-Tg, GFP	6/6	75.1 ± 3.4	5/5	74.7 ± 2.5
Wt-Tg, αSyn	6/7	74.3 ± 7.1	6/6	74.4 ± 4.2
I93M-Tg, GFP	4/6	68.2 ± 2.1	7/7	80.8 ± 1.5
I93M-Tg, αSyn	5/6	75.2 ± 7.9	6/7	70.4 ± 5.1
Non-Tg, αSyn	4/6	76.6 ± 5.9	5/6	68.8 ± 4.6

Mice, rAAV1	3-month-old, 4-week post-injection		3-month-old, 8-week post-injection		3-month-old, 13-week post-injection	
	Number of mice	Efficiency (%)	Number of mice	Efficiency (%)	Number of mice	Efficiency (%)
wild-type, GFP	4/4	77.6 ± 0.9	5/5	79.4 ± 5.9	5/5	76.1 ± 3.7
wild-type, αSyn	4/4	74.8 ± 1.0	5/5	73.2 ± 4.8	6/6	77.2 ± 4.6
gad, GFP	5/5	75.7 ± 0.9	5/5	77.7 ± 9.8	6/6	67.5 ± 2.1
gad, αSyn	5/5	76.1 ± 1.1	5/5	80.4 ± 6.4	7/7	77.2 ± 2.1

[a]Data are number of mice selected for DA cell count over that of total mice injected with rAAV1 vector.
[b]Transduction efficiency of rAAV1 vector was expressed as percentage of total DA cells in the SNpc; *i.e.*, the number of DA cells in the contralateral uninjected side in the area immunopositive for foreign protein relative to that in the entire rostrocaudal extent of the SNpc (mean ± SEM).
Wt-Tg, UCH-L1$^{wild\text{-}type}$-Tg; I93M-Tg, UCH-L1^{Ile93Met}-Tg.

concentration in the rAAV1-injected side over that in the intact side. One-way analysis of variance (ANOVA) followed by Tukey-Kramer's *post hoc* test was applied to evaluate the statistical differences among the groups. A p value less than 0.05 denoted the presence of statistically significant difference.

Results

Co-localization of αSyn and UCH-L1 proteins in nigral Lewy bodies in human PD brain

At first, we performed immunohistochemical analysis for αSyn and UCH-L1 proteins using a midbrain section of a patient with sporadic PD. We found several αSyn- and UCH-L1-double-positive Lewy bodies in the pigmented DA cells in the SN (Fig. 1). αSyn and UCH-L1 proteins co-localized on the halo of Lewy bodies. No fluorescent labeling was detected in the control staining lacking the primary antibodies (data not shown). These results suggested a potential physical and/or functional interaction between the two proteins in human PD brain and prompted us to examine this issue in the experimental animal model of PD.

rAAV1 vector-mediated expression of hrGFP or human αSyn protein in mouse DA neurons

The high-titer viral stocks of rAAV1-hrGFP (6×10^{11} genomes/mL) and rAAV1-αSyn (6×10^{11} genomes/mL) were prepared and injected unilaterally into the SN of 3-month-old UCH-L1$^{wild\text{-}type}$-Tg, UCH-L1^{Ile93Met}-Tg mice, and their non-Tg littermates. At 4-weeks post-injection period, mice were killed and examined for the expression of foreign proteins in the SN by immunohistochemical analysis (Fig. 2). We used a polyclonal antibody that detects hrGFP (green; Fig. 2a–d), a monoclonal antibody (clone LB509) that specifically detects αSyn protein of human origin (green; Fig. 2e–j), and anti-TH antibody that stains DA neurons (red; Fig. 2b, d, f, h, and j). The hrGFP protein was distributed uniformly in DA cell bodies (Fig. 2a and c, arrows) and neuronal processes (Fig. 2a and c, arrowheads) in the SNpc of UCH-L1$^{wild\text{-}type}$-Tg (Fig. 2a and b) and UCH-L1^{Ile93Met}-Tg mice (Fig. 2c and d). On the other hand, virally-introduced human αSyn protein was localized in the cytoplasm, processes (Fig. 2e, g, and i, arrowheads), and perinuclear region (Fig. 2e, g, and i, asterisks) of DA neurons in the SNpc of UCH-L1$^{wild\text{-}type}$-Tg (Fig. 2e and f), UCH-L1^{Ile93Met}-Tg mice (Fig. 2g and h), and non-Tg littermates (Fig. 2i and j). Immunoreactivity for human αSyn was also detected in the intranuclear space in all mice groups (co-localized with DAPI, data not shown), and no major differences were found in the distribution of αSyn protein among the groups. A similar distribution of virally-introduced αSyn was observed in the SNpc DA neurons of 12-month-old Tg and non-Tg mice (data not shown).

Importantly, densitometric analysis of human αSyn in single SNpc cells in these mice showed a significantly higher

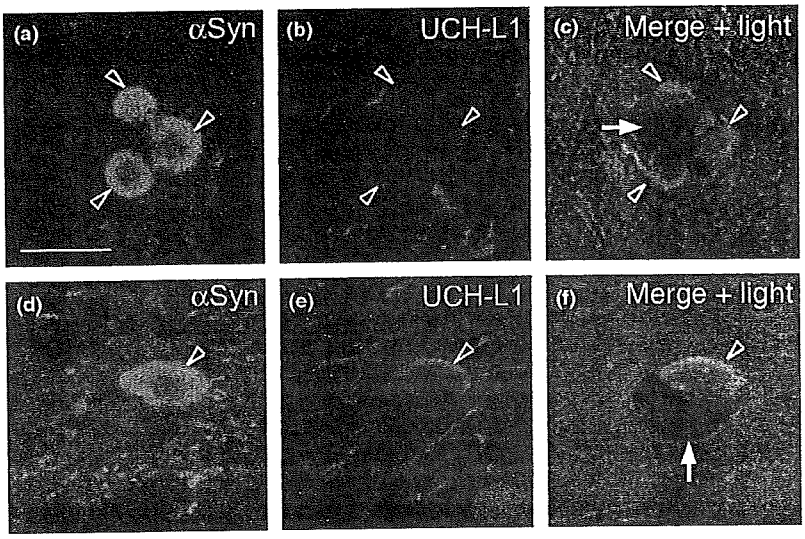

Fig. 1 Immunohistochemical analysis of αSyn and UCH-L1 proteins in the SN of human PD patient. A representative midbrain section of a patient with sporadic PD was immunostained for αSyn (green; a and d) and UCH-L1 proteins (red; b and e). Images were captured using a confocal laser-scanning microscope. Note that several Lewy bodies formed in the pigmented DA neurons (c and f; indicated by white arrows) were double-positive for αSyn and UCH-L1 proteins (a–f; open arrowheads). Scale bar in (a), 20-μm (applicable to a–f).

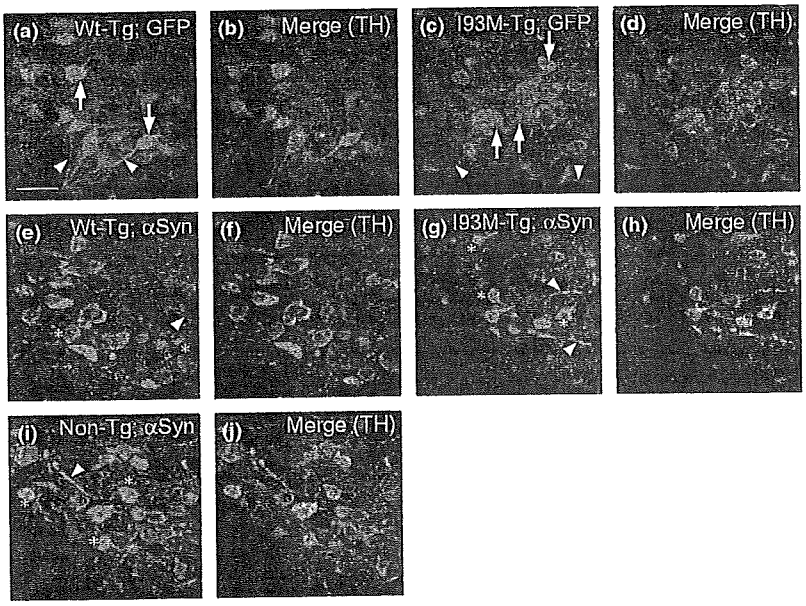

Fig. 2 Recombinant adeno-associated virus (rAAV)-mediated expression of hrGFP and human αSyn protein in mouse DA neurons in the SNpc. The distribution patterns of hrGFP (green; a–d) and αSyn protein (green; e–j) were analyzed in UCH-L1$^{wild\text{-}type}$-Tg (a, b, e, and f; denoted as Wt-Tg), UCH-L1^{Ile93Met}-Tg (c, d, g, and h; I93M-Tg), and non-Tg (i and j; Non-Tg) mice. The DA cell bodies are detected by anti-TH immunostaining (red; b, d, f, h, and j). While hrGFP protein shows a uniform distribution in DA cells and processes (a–d), αSyn is found in cytoplasm, processes (e–j, arrow heads), and perinuclear region (e–j, asterisks) of DA neurons. There are no major differences in the distribution of αSyn among all types of mice examined. Scale bar in (a), 50-μm (applicable to a–j).

immunoreactivity for αSyn in UCH-L1^{Ile93Met}-Tg mice than in UCH-L1$^{wild\text{-}type}$-Tg and non-Tg mice (Fig. 3a–d).

Next, we injected rAAV1-hrGFP or rAAV1-αSyn into the SN of 3-month-old *gad* mice and their wild-type littermates. Similarly, hrGFP protein was distributed uniformly in DA cell bodies and neuronal processes, and αSyn protein was identified in the cytoplasm, processes, perinuclear region, and intranuclear spaces of DA neurons in the SNpc of these mice with no significant difference between the groups (data not shown). As shown in Fig. 4(a)–(c), there was no significant difference in the virally-expressed αSyn between the groups at 13-weeks post-injection, as confirmed by densitometric analysis.

Effect of αSyn over-expression in UCH-L1-Tg mice

Next, we studied the effect of αSyn over-expression on the survival of DA neurons in Tg and non-Tg mice. Every fourth 20-μm-thick serial nigral section was immunostained using anti-TH antibody, followed by Nissl staining. As shown in Fig. 5, loss of DA cell bodies was observed in the SNpc of UCH-L1^{Ile93Met}-Tg mice injected with rAAV1-αSyn (compare Fig. 5e and f, and g and h; indicated by open arrowheads in e) at 4-weeks post-injection. On the other hand, injection of rAAV1-αSyn caused no apparent cell loss in UCH-L1$^{wild\text{-}type}$-Tg (Fig. 5a–d) and non-Tg mice (Fig. 5i–l) at the same time point. Immunostaining for another DA cell marker, dopamine transporter, also showed loss of DA

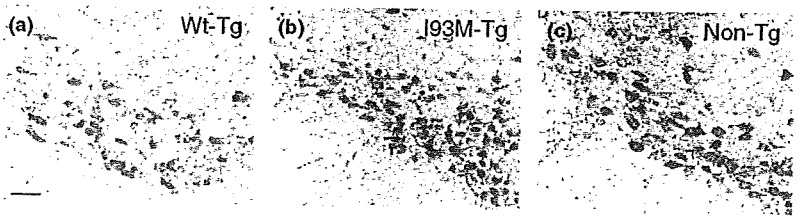

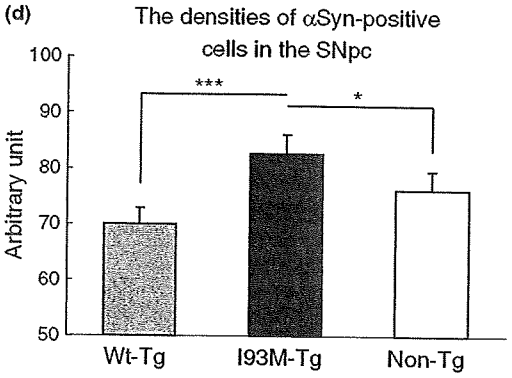

Fig. 3 Densitometric quantification of αSyn in single cells of the SNpc of UCH-L1-Tg and non-Tg mice. Nigral sections were subjected to anti-human αSyn immunostaining. Representative photographs were taken in UCH-L1$^{wild\text{-}type}$-Tg (a; denoted as Wt-Tg), UCH-L1^{Ile93Met}-Tg (b; I93M-Tg), and non-Tg mice (c; Non-Tg). Scale bar in (a), 50-μm (applicable to a–c). (d) The density of human αSyn was quantified using 4–7 of every four serial nigral sections (n = 4 mice for each group). $^{*}p < 0.05$ and $^{***}p < 0.001$ (two-tailed Student's t-test).

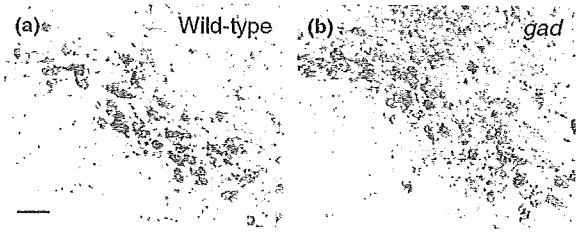

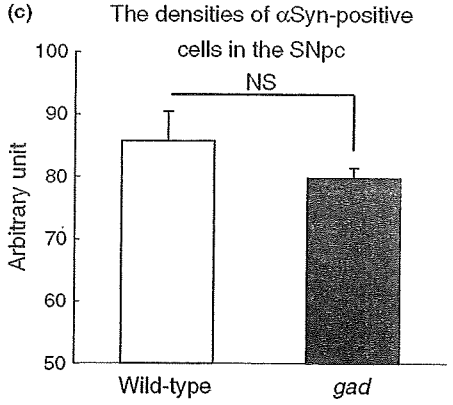

Fig. 4 Densitometric quantification of αSyn in single cells of the SNpc of wild-type and *gad* mice. Nigral sections were subjected to anti-human αSyn immunostaining. Representative photographs were taken in wild-type (a) and *gad* mice (b). Scale bar in (a), 50-μm (applicable to a and b). (c) The density of human αSyn was quantified using 4–7 of every four serial nigral sections (n = 4 mice for each group). n.s., not significant (two-tailed Student's t-test).

cell bodies in the SNpc of UCH-L1^{Ile93Met}-Tg mice injected with rAAV1-αSyn (Fig. 6a–f). Immunostaining of nigral sections of the three genetic types of mice using anti-active caspase-3 antibody showed anti-active caspase-3-immunoreactivities in the SNpc of the rAAV1-αSyn-injected side of UCH-L1^{Ile93Met}-Tg mice (Fig. 6g). These results suggest that αSyn-induced DA cell degeneration in UCH-L1^{Ile93Met}-Tg mice is mediated through apoptotic machinery. Then, we counted the number of TH- and Nissl-positive SNpc cells in both rAAV1-injected and non-injected intact sides of these mice. Immunostaining in the rostrocaudal areas of the SN for hrGFP and human αSyn varied among mice, and accordingly, we determined the immunostaining in each mouse using every eighth 20-μm-thick serial nigral section. Mice positive for the virally-introduced protein in more than half of the rostrocaudal region of the SN were selected for DA cell counting (see Materials and Methods). Table 1 provides a summary of the numbers of selected mice, rAAV1-injected mice, and transduction efficiencies of rAAV1 vector in the selected mice. In Fig. 7(a) and (b), the data are represented as % of contralateral, *i.e.*, TH- and Nissl-positive cell number in the rAAV1-injected side relative to that in the intact side. In rAAV1-αSyn-injected mice (Fig. 7a and b, solid bars), UCH-L1^{Ile93Met}-Tg mice (n = 5, number of animals shown in parenthesis in each bar) exhibited significant loss of DA cell bodies (~30% decrease) compared with UCH-L1$^{wild\text{-}type}$-Tg (~0% decrease) and non-Tg mice (~10% decrease). Furthermore, the relative number of DA cells in the rAAV1-αSyn-injected UCH-L1^{Ile93Met}-Tg mice was significantly lower than in rAAV1-hrGFP-injected UCH-L1^{Ile93Met}-Tg mice (Fig. 7a and b, open bars; ~0% decrease), indicating that the loss of DA cell bodies was mediated specifically by αSyn protein but not by the rAAV1 vector itself or surgical injury. In 12-month-old UCH-L1^{Ile93Met}-Tg mice, we observed a similar extent (~30% decrease) of significant degeneration of TH- and Nissl-positive DA cell bodies,

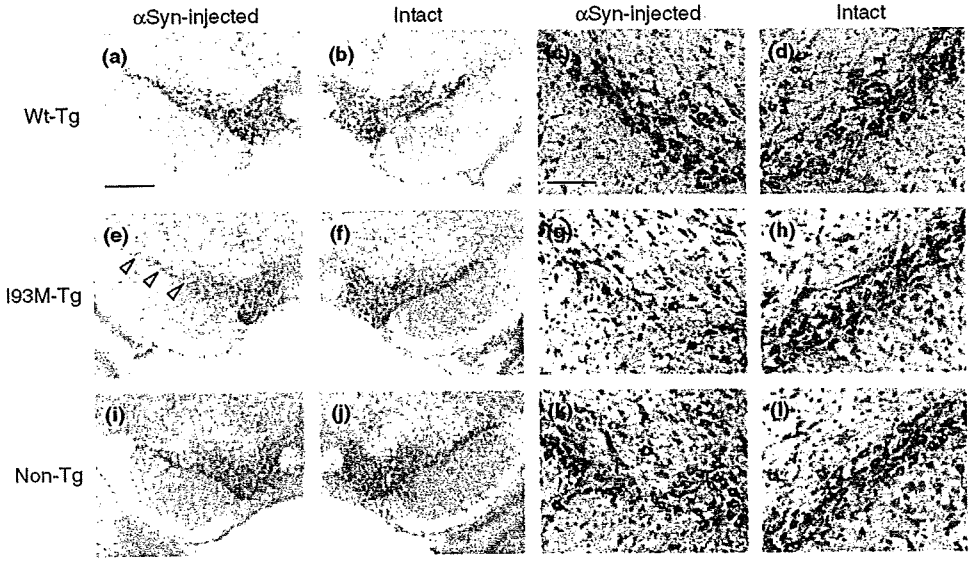

Fig. 5 α-Synuclein-induced degeneration of DA cell bodies in the SNpc of UCH-L1^{Ile93Met}-Tg mice at 4-weeks post-injection. Nigral sections were subjected to anti-TH immunostaining, followed by Nissl staining. Photographs were taken in UCH-L1$^{wild\text{-}type}$-Tg (a–d; denoted as Wt-Tg), UCH-L1^{Ile93Met}-Tg (e–h; I93M-Tg), and non-Tg mice (i–l; Non-Tg) injected with rAAV1-αSyn. The rAAV1-αSyn-injected side (a, c, e, g, i, and k; αSyn-injected) and non-injected intact side (b, d, f, h, j, and l; Intact) are shown. Panels (c), (d), (g), (h), (k), and (l) are enlarged images of (a), (b), (e), (f), (i), and (j), respectively. Note that the DA cell bodies are degenerated in UCH-L1^{Ile93Met}-Tg mice (compare e and f, and g and h; indicated by open arrowheads in e). Scale bar in (a), 500-μm (applicable to a, b, e, f, i, and j); and in (c), 100-μm (to c, d, g, h, k, and l).

which was also specifically induced by αSyn over-expression (Fig. 7a and b).

Next, we measured striatal dopamine concentrations in these mice. However, we could not detect any significant decrease in dopamine concentrations, both in 3- and 12-month-old mice, between the rAAV1-hrGFP- (Fig. 7c, open bars; % of contralateral) and rAAV1-αSyn-injected groups (solid bars) in both UCH-L1$^{wild\text{-}type}$-Tg and UCH-L1^{Ile93Met}-Tg mice, and among the three genetic types of mice in the rAAV1-αSyn-injected groups. There were also no significant changes in the concentrations of dopamine metabolites; DOPAC and HVA (data not shown).

Effects of αSyn over-expression in *gad* mice

Finally, we investigated the effect of viral introduction of αSyn in *gad* and their wild-type littermates. The rAAV1-injected mice were selected for the following investigations based on the criteria described above (see also Table 1). At 13-weeks post-injection period, anti-TH- and Nissl-double-staining of nigral sections manifested an rAAV1-αSyn-induced decrease of DA cell bodies in the SNpc of *gad* (Fig. 8e–h) and wild-type mice (Fig. 8a–d). When the number of the SNpc DA cell bodies was counted, we found that the rAAV1-αSyn-induced DA cell loss was significant both in *gad* and wild-type mice at 13-weeks post-injection period (Fig. 9a and b). We also found that there were no significant differences between the rAAV1-αSyn-injected *gad* and wild-type groups at 4- (~10% decrease, Fig. 9a and b), 8- (~20% decrease), and 13-weeks post-injection (~25% decrease), while the rAAV1-αSyn-induced DA cell loss was not yet significant in *gad* mice compared with the rAAV1-hrGFP-injected group at 8-weeks post-injection.

There was no significant decrease in striatal dopamine concentrations at both 8- and 13-weeks post-injection, between the rAAV1-hrGFP- (Fig. 9c, open bars; % of contralateral) and rAAV1-αSyn-injected groups (solid bars), in both wild-type and *gad* mice, and between wild-type and *gad* mice in the rAAV1-αSyn-injected groups. Furthermore, the level of dopamine metabolites, DOPAC and HVA, were not changed in all groups (data not shown).

Discussion

In the present study, based on the previous findings that αSyn and UCH-L1 proteins interact physically in a cell model of PD (Zhou *et al.* 2004) and normal mammalian brain (Liu *et al.* 2002), and are deposited in Lewy bodies in sporadic cases of PD (Lowe *et al.* 1990; Spillantini *et al.* 1997; Baba *et al.* 1998), we performed a fluorescent double-immunolabeling analysis for the two proteins using a midbrain section of a patient with sporadic PD. Co-localization of αSyn and UCH-L1 proteins in the halo of several Lewy bodies (Fig. 1) encouraged us to examine the potential functional interaction between the two proteins in a mouse model of PD; in

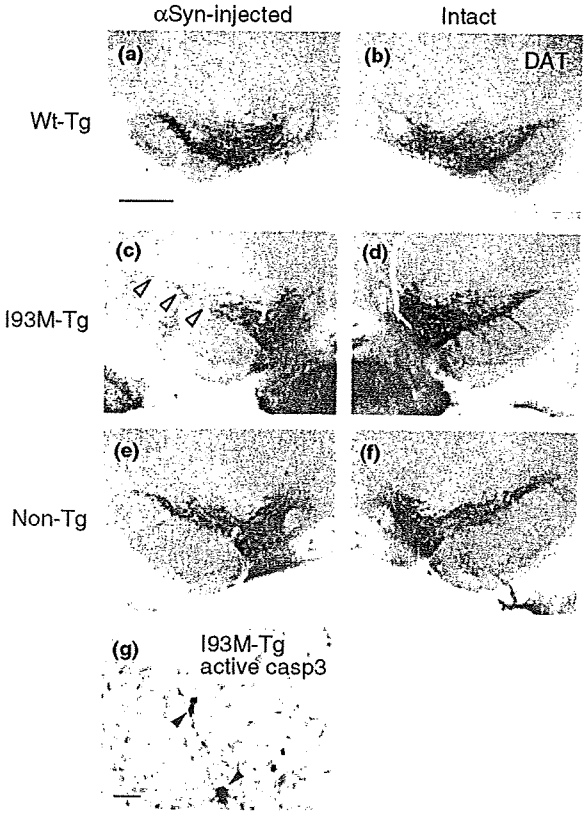

Fig. 6 α-Synuclein-induced degeneration of DA cell bodies examined by anti-DAT- and anti-active caspase-3-immunostaining. Photographs of anti-DAT immunostaining were taken in UCH-L1$^{wild\text{-}type}$-Tg (a, b; denoted as Wt-Tg), UCH-L1^{Ile93Met}-Tg (c, d; I93M-Tg), and non-Tg mice (e, f; Non-Tg) injected with rAAV1-αSyn. The rAAV1-αSyn-injected side (a, c, and e; αSyn-injected) and non-injected intact side (b, d, and f; Intact) are shown. Note the degenerated DA cell bodies in UCH-L1^{Ile93Met}-Tg mice (compare c and d; open arrowheads in c). Immunoreactivity for active caspase-3 (active casp3) is present in the SNpc of UCH-L1^{Ile93Met}-Tg mice injected with rAAV1-αSyn (g; solid arrowheads). Sections were subjected to Nissl counter-staining. Scale bar in (a), 500-μm (applicable to a–f); and in (g) 25-μm.

particular, whether UCH-L1 affects DA neurotoxicity of abnormally accumulated αSyn protein. The αSyn immunoreactivity on the halo of Lewy bodies was consistent with a previous report, which showed localization of αSyn at peripheral portions of Lewy bodies by immunoelectron microscopic analysis (Baba *et al.* 1998). We investigated αSyn-induced DA neurodegeneration in UCH-L1-Tg and -null mice by using the rAAV-mediated gene delivery. In the 4-week-period of rAAV1-mediated αSyn over-expression (shown in Figs 2 and 3), immunoreactivities for human αSyn in single SNpc cells increased significantly in UCH-L1^{Ile93Met}-Tg mice compared with UCH-L1$^{wild\text{-}type}$-Tg and non-Tg mice (Fig. 3). In this regard, we recently reported that the UCH-L1^{Ile93Met} protein inhibits chaperone-mediated autophagy through abnormally enhanced interaction between the UCH-L1 mutant and LAMP-2A protein (Kabuta and Wada 2008; Kabuta *et al.* 2008a). Such abnormal function of UCH-L1^{Ile93Met} protein might have influenced the accumulation of αSyn in the present model. Furthermore, the loss of DA cell bodies was significantly enhanced in the SNpc of UCH-L1^{Ile93Met}-Tg mice, while it was not yet apparent in UCH-L1$^{wild\text{-}type}$-Tg and non-Tg mice at 4-weeks post-injection (Figs 5–7). We also found that αSyn-induced DA neurodegeneration in UCH-L1^{Ile93Met}-Tg mice occurred through an apoptotic mechanism (Fig. 6). In a pilot experiment, we found a significant decrease in the number of nigral DA cell bodies at 8- and 13-weeks post-injection of rAAV1-αSyn, but the number was not significantly different from that of UCH-L1$^{wild\text{-}type}$-Tg, UCH-L1^{Ile93Met}-Tg, and non-Tg mice. Thus, the present results indicate that the DA neurotoxicity of αSyn protein is markedly enhanced in the presence of UCH-L1^{Ile93Met} protein. Furthermore, we found that αSyn over-expression at 13 weeks (Fig. 4) was associated with a significant DA neurodegeneration in *gad* mice, although the extent of DA cell loss was not significantly different than their wild-type littermates (Figs 8 and 9). These results indicate that the αSyn protein-induced DA neurotoxicity is not altered in the absence of UCH-L1$^{wild\text{-}type}$ protein. The striatal levels of dopamine and its metabolites, DOPAC and HVA, did not change during the period of our study (Figs 7c and 9c). In a recent study, Gorbatyuk *et al.* (2008) reported that serotype-5 rAAV-mediated over-expression of human wild-type αSyn caused a significant decrease in the number of TH- and Nissl-positive cells in the SNpc of rats at 8-weeks post-injection, while the striatal level of dopamine showed no significant decrease. Such discrepancy in the rodent models may because of the difficulty of rAAV particles to fully infiltrate the entire rostrocaudal part of the SN (Table 1), as we have suggested in a previous study (Yamada *et al.* 2004). Alternatively, the relatively slow progression of DA neurodegeneration in this model, compared with other drug-induced PD animal models, might have enabled a feedback overproduction of dopamine in the surviving and/or uninfected DA neurons.

Initially, it was reported that the *PARK5*-associated UCH-L1^{Ile93Met} mutant results in ~50% decrease in its ubiquitin hydrolase activity (Leroy *et al.* 1998; Nishikawa *et al.* 2003). Considered with the fact that *PARK5* has so far been identified in only one German kindred, without absolute penetration (Leroy *et al.* 1998), it is debatable whether *PARK5* is caused by a dominant gain-of-toxic-function or haploinsufficiency, *i.e.*, loss-of-function. In this regard, our recent study showed an age-dependent nigrostriatal DA neurodegeneration in a Tg mice line over-expressing human UCH-L1^{Ile93Met} protein (Setsuie *et al.* 2007). Although the level of transgene expression in the UCH-L1^{Ile93Met}-Tg mice line decreased gradually with aging (Setsuie *et al.* 2007) and the number of nigral DA cell bodies in aged UCH-L1^{Ile93Met}-

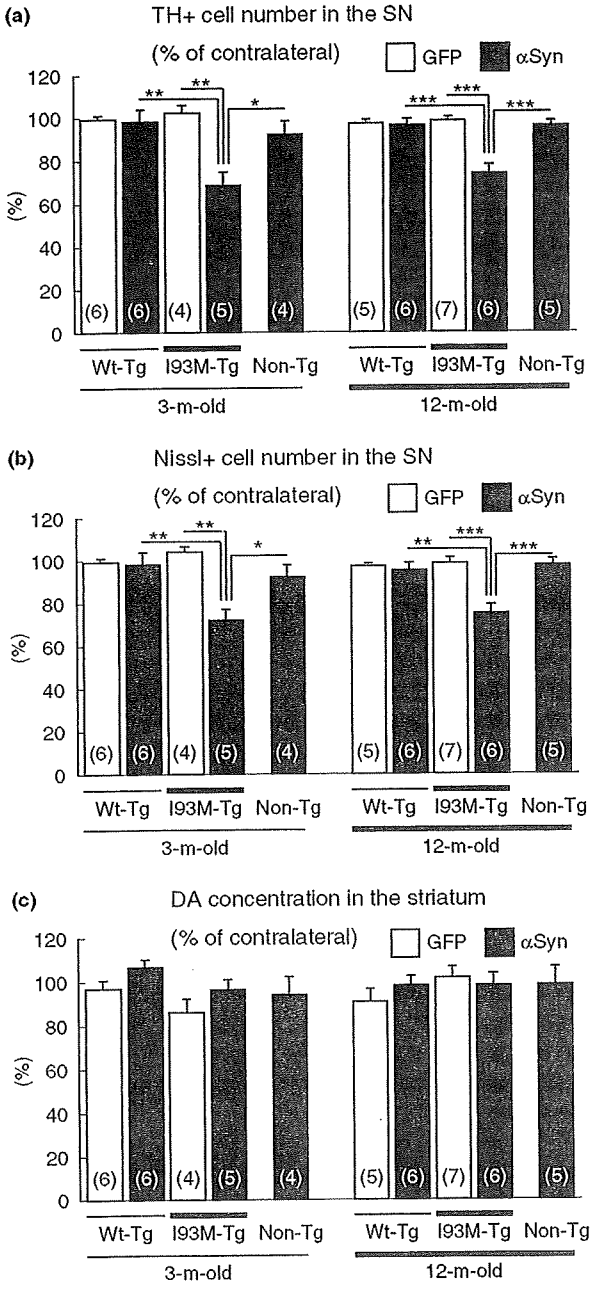

Fig. 7 Dopaminergic cell numbers in the SNpc and dopamine levels in the striatum of UCH-L1-Tg and non-Tg mice at 4-weeks post-injection. The TH- (a) and Nissl-positive cells (b) in the SNpc were counted in 3- and 12-month-old UCH-L1$^{\text{wild-type}}$- (Wt-Tg), UCH-L1$^{\text{Ile93Met}}$-Tg (I93M-Tg), and non-Tg mice (Non-Tg). Data are % of those in the contralateral side. *Open bars:* rAAV1-hrGFP-injected groups, *solid bars:* rAAV1-αSyn-injected groups. The number of analyzed mice in each group is indicated within the bars. Data are mean ± SEM. $^{*}p < 0.05$, $^{**}p < 0.01$, and $^{***}p < 0.001$ (one-way ANOVA followed by Tukey-Kramer's *post hoc* test). Note that the numbers of DA cells are significantly lower in rAAV1-αSyn-injected UCH-L1$^{\text{Ile93Met}}$-Tg mice than in UCH-L1$^{\text{wild-type}}$-Tg and non-Tg mice both in 3- and 12-month-old mice. Significant differences were also found between the rAAV1-hrGFP- and rAAV1-αSyn-injected groups in UCH-L1$^{\text{Ile93Met}}$-Tg mice both at 3- and 12-months of age. (c) The striatal levels of dopamine measured in rAAV1-injected mice. Data are % of those in the contralateral side. *Open bars:* rAAV1-hrGFP-injected groups, *solid bars:* rAAV1-αSyn-injected groups. The number of analyzed mice in each group is indicated within the bars. Data are mean ± SEM. There were no significant differences in dopamine levels among the examined groups.

Tg mice was not significantly different from age-matched non-Tg littermates (data not shown), our present investigation demonstrated that the rAAV1-αSyn-induced DA cell loss was not influenced by the age of UCH-L1$^{\text{Ile93Met}}$-Tg mice. These results also suggest that the DA neurotoxicity of UCH-L1$^{\text{Ile93Met}}$ protein alone might be relatively weak in the absence of abnormal accumulation of αSyn. In this regard, a recent study showed no significant change in endogenous αSyn in UCH-L1$^{\text{Ile93Met}}$-Tg mice (Setsuie *et al.* 2007). Based on the finding that the normal aging process is associated with a significant accumulation of αSyn protein in the SN of human brain (Li *et al.* 2004; Chu and Kordower 2007), we speculate that the toxicity of accumulated αSyn might be enhanced by the UCH-L1$^{\text{Ile93Met}}$ protein in *PARK5* carriers, leading to a critical loss of DA cells and subsequent development of PD symptoms. The precise mechanism for mutated UCH-L1-mediated toxicity in the presence of accumulated αSyn should be clarified in future studies.

Several studies have reported that the over-expressed αSyn functions as a protective molecule in neuronal cells other than DA neurons (da Costa *et al.* 2000; Xu *et al.* 2002; Chandra *et al.* 2005). The selective vulnerability of DA cells in PD could be explained by the findings that αSyn protein could be covalently bound to dopamine (Conway *et al.* 2001) or could be conformationally changed by interaction with dopaminochrome *in vitro* (Norris *et al.* 2005). Both these mechanisms could lead to altered aggregation propensity, exerting a selective toxicity against culture DA cells (Xu *et al.* 2002), and elevation of intracellular catecholamine level (Mosharov *et al.* 2006). UCH-L1 is also reported to undergo oxidative modification in the brains of patients with PD and Alzheimer's disease (Choi *et al.* 2004). Furthermore, we reported recently that carbonyl-modified UCH-L1 shares aberrant molecular properties with UCH-L1$^{\text{Ile93Met}}$, including similar secondary structural changes, increased insolubility, and elevated interaction with various proteins such as tubulin (Kabuta *et al.* 2008b). We speculate that such post-translational modification, or perhaps another yet unidentified modification(s), could potentially induce the neurotoxic activity of UCH-L1, rendering the accumulated αSyn protein neurotoxic to nigral DA neurons in patients with the sporadic form of PD.

On the other hand, our present study showed that nigral DA cells were killed to no more/lesser extent by the

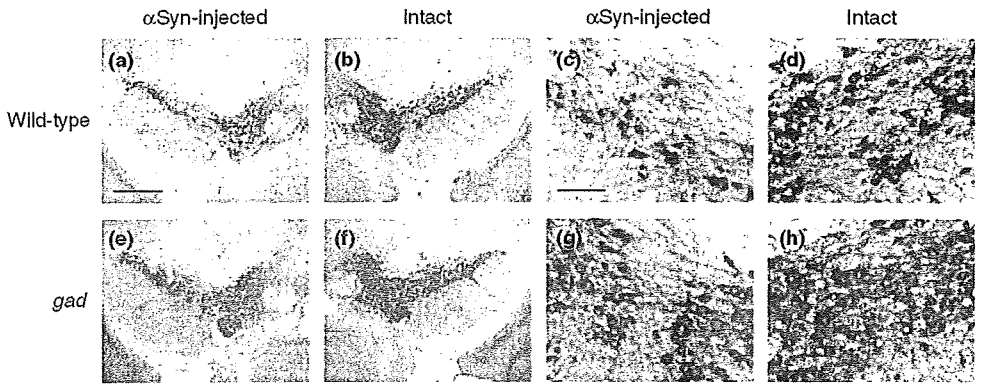

Fig. 8 α-Synuclein-induced degeneration of DA cell bodies in the SNpc of wild-type and *gad* mice at 13-weeks post-injection. Nigral sections were subjected to anti-TH immunostaining, followed by Nissl staining. Photographs were taken in wild-type littermate (a–d) and *gad* mice (e–h) injected with rAAV1-αSyn. The rAAV1-αSyn-injected side (a, c, e, and g; αSyn-injected) and non-injected intact side (b, d, f, and h; Intact) are shown. Panels (c), (d), (g), and (h) are enlarged images of (a), (b), (e), and (f), respectively. Note the degeneration of DA cell bodies in the rAAV1-αSyn-injected sides in both the wild-type and *gad* mice. Scale bar in (a), 500-μm (applicable to a, b, e, and f); and in (c), 100-μm (to c, d, g, and h).

injection of rAAV1-αSyn in the absence of UCH-L1 protein, *i.e.*, in *gad* mice. Previous pathological studies in *gad* mice suggested that UCH-L1 has important roles in the survival of certain neuronal populations, such as sensory and motor neurons (Oda *et al.* 1992; Miura *et al.* 1993). Recent reports also showed that UCH-L1 protein is involved in the survival of other types of neuronal cells. In birds and mice, up-regulation of UCH-L1 is associated with increased survival of replaceable neurons, which continue to be produced and replaced in adulthood (Lombardino *et al.* 2005). Moreover, transduction of exogenous UCH-L1 protein protected against β-amyloid-induced synaptic dysfunction of hippocampal neurons *in vitro* and improved the retention of contextual learning in a mouse model of Alzheimer's disease (Gong *et al.* 2006). As mentioned above, UCH-L1 protein is oxidatively modified and down-regulated in the frontal cortex of patients with sporadic PD and Alzheimer's disease (Choi *et al.* 2004). We reported that oxidation of UCH-L1 protein by 4-hydroxynonenal resulted in a loss of ubiquitin hydrolase activity *in vitro* (Nishikawa *et al.* 2003). In another study, we also reported that UCH-L1 bound to and stabilized monomeric ubiquitin molecule *in vivo*; the level of monomeric ubiquitin was significantly decreased in various brain structures of *gad* mice (Osaka *et al.* 2003). Moreover, proteomic analysis of proteins isolated from the cortical area of *gad* brain revealed oxidative modification of several key proteins possibly linked to neurodegeneration (Castegna *et al.* 2004). However, it is still unknown whether such modification of proteins does occur in the nigral DA cells of *gad* mice. Indeed, no pathological changes have been reported in the SN of *gad* mice. When we counted the number of TH- and Nissl-double-positive DA cells in the entire rostrocaudal extent of the SNpc of *gad* mice, there was no significant difference with wild-type mice (data not shown). Thus, we add an alternative scenario; functional loss of UCH-L1 might have neuroprotective effects. The present study showed that there was no significant decrease in DA cells in *gad* mice between rAAV1-hrGFP-injected and rAAV1-αSyn-injected groups at 8-weeks post-injection, while there was a significant one in wild-type mice (Fig. 9a and b). These results could imply the potential deleterious effects of normal UCH-L1, which were suggested previously by Liu *et al.* (2002). Recently, we reported that retinal neurons in *gad* mice were resistant to ischemic injury (Harada *et al.* 2004). Ischemic stress induces UCH-L1-mediated up-regulation of ubiquitin in wild-type mice, but high levels of ubiquitin induced caspase-dependent retinal neuronal apoptosis (Harada *et al.* 2004). We speculate that another closely related ubiquitin hydrolyzing enzyme, UCH-L3, might have complemented the loss of UCH-L1. The UCH-L1- and UCH-L3-double-null mice show more severe neurodegenerative phenotypes than *gad* mice (Kurihara *et al.* 2001); accordingly, the vulnerability of their nigrostriatal DA neurons to αSyn accumulation should be analyzed in detail in the future. However, the present results demonstrated clearly that the loss of UCH-L1 protein does not cause any harmful or protective effect on prolonged abnormal accumulation of αSyn in nigral DA cells.

In conclusion, our study showed that accumulated αSyn protein is neurotoxic to DA neurons and that such neurotoxicity is enhanced by *PARK5*-associated UCH-L1^{Ile93Met} mutant, but not influenced by the loss of UCH-L1$^{wild\text{-}type}$ protein *in vivo*. Accordingly, we believe that the present results support the hypothesis of dominant gain-of-toxic-function mutation of UCH-L1 as the cause of *PARK5*. Considering the possibility that the UCH-L1$^{wild\text{-}type}$ protein might be toxic by certain age-dependent post-translational

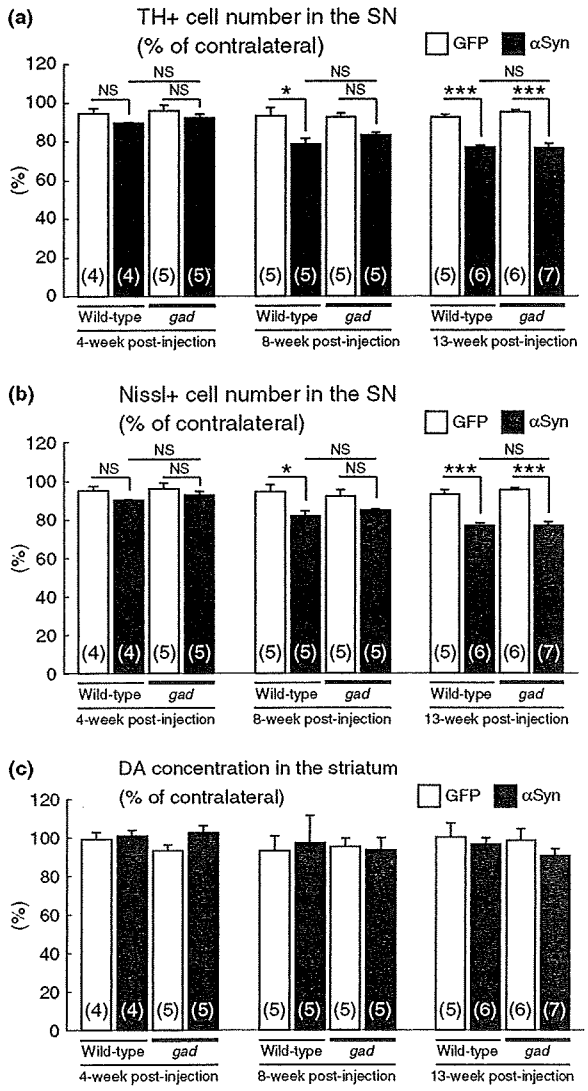

Fig. 9 Dopaminergic cell number in the SNpc and dopamine concentration in the striatum of wild-type and *gad* mice at 4-, 8-, and 13-weeks post-injection. The TH- (a) and Nissl-positive cells (b) in the SNpc were counted in 3-month-old mice. Data are % of the numbers in the contralateral side. *Open bars:* rAAV1-hrGFP-injected groups, *solid bars:* rAAV1-αSyn-injected groups. The number of analyzed mice in each group is indicated within the bars. Data are mean ± SEM. $^{*}p < 0.05$, $^{***}p < 0.001$, and n.s., not significant (one-way ANOVA followed by Tukey-Kramer's *post hoc* test). Note the lack of significant differences between the rAAV1-αSyn-injected wild-type and *gad* groups both at 8- and 13-weeks post-injection. (c) The striatal levels of dopamine were measured in the rAAV1-injected mice. Data are % of the levels in the contralateral side. *Open bars:* rAAV1-hrGFP-injected groups, *solid bars:* rAAV1-αSyn-injected groups. The number of analyzed mice in each group is indicated within the bars. Data are mean ± SEM. There were no significant differences in dopamine levels in the examined groups.

modifications in DA neurons, elucidation of the entire functions of fPD-linked causative gene products and functional interactions among them should provide new insights into the molecular pathogenesis and clinical approaches for the sporadic form of PD.

Acknowledgements

This work was supported by a High Technology Research Center grant, Program for Promotion of Fundamental Studies in Health Sciences of the National Institute of Biomedical Innovation, a Grant-in-Aid for Scientific Research from the Ministry of Education, Culture, Sports, Science and Technology of Japan, and a Grant-in-Aid for Scientific Research from the Ministry of Health, Labour and Welfare of Japan.

References

Baba M., Nakajo S., Tu P. H., Tomita T., Nakaya K., Lee V. M., Trojanowski J. Q. and Iwatsubo T. (1998) Aggregation of alpha-synuclein in Lewy bodies of sporadic Parkinson's disease and dementia with Lewy bodies. *Am. J. Pathol.* **152**, 879–884.

Castegna A., Thongboonkerd V., Klein J., Lynn B. C., Wang Y. L., Osaka H., Wada K. and Butterfield D. A. (2004) Proteomic analysis of brain proteins in the gracile axonal dystrophy (gad) mouse, a syndrome that emanates from dysfunctional ubiquitin carboxyl-terminal hydrolase L-1, reveals oxidation of key proteins. *J. Neurochem.* **88**, 1540–1546.

Chandra S., Gallardo G., Fernandez-Chacon R., Schluter O. M. and Sudhof T. C. (2005) Alpha-synuclein cooperates with CSPalpha in preventing neurodegeneration. *Cell* **123**, 383–396.

Choi J., Levey A. I., Weintraub S. T., Rees H. D., Gearing M., Chin L. S. and Li L. (2004) Oxidative modifications and down-regulation of ubiquitin carboxyl-terminal hydrolase L1 associated with idiopathic Parkinson's and Alzheimer's diseases. *J. Biol. Chem.* **279**, 13256–13264.

Chu Y. and Kordower J. H. (2007) Age-associated increases of alpha-synuclein in monkeys and humans are associated with nigrostriatal dopamine depletion: is this the target for Parkinson's disease? *Neurobiol. Dis.* **25**, 134–149.

Conway K. A., Rochet J. C., Bieganski R. M. and Lansbury P. T. Jr (2001) Kinetic stabilization of the alpha-synuclein protofibril by a dopamine-alpha-synuclein adduct. *Science* **294**, 1346–1349.

da Costa C. A., Ancolio K. and Checler F. (2000) Wild-type but not Parkinson's disease-related ala-53 –> Thr mutant alpha-synuclein protects neuronal cells from apoptotic stimuli. *J. Biol. Chem.* **275**, 24065–24069.

Farrer M. J. (2006) Genetics of Parkinson disease: paradigm shifts and future prospects. *Nat. Rev. Genet.* **7**, 306–318.

Furuya T., Hayakawa H., Yamada M., Yoshimi K., Hisahara S., Miura M., Mizuno Y. and Mochizuki H. (2004) Caspase-11 mediates inflammatory dopaminergic cell death in the 1-methyl-4-phenyl-1,2,3,6-tetrahydropyridine mouse model of Parkinson's disease. *J. Neurosci.* **24**, 1865–1872.

Gong B., Cao Z., Zheng P., Vitolo O. V., Liu S., Staniszewski A., Moolman D., Zhang H., Shelanski M. and Arancio O. (2006) Ubiquitin hydrolase Uch-L1 rescues beta-amyloid-induced decreases in synaptic function and contextual memory. *Cell* **126**, 775–788.

Gorbatyuk O. S., Li S., Sullivan L. F., Chen W., Kondrikova G., Manfredsson F. P., Mandel R. J. and Muzyczka N. (2008) The

